

## ELECTRONIC SUPPLEMENTARY INFORMATION

### Characterization of Secondary Phosphine Oxide Ligands on the Surface of Iridium Nanoparticles

Israel Cano,<sup>\*a</sup> Luis M. Martínez-Prieto,<sup>a</sup> Pier F. Fazzini,<sup>a</sup> Yannick Coppel,<sup>b</sup> Bruno Chaudret,<sup>a</sup>  
and Piet W. N. M. van Leeuwen<sup>\*a</sup>

<sup>a</sup>Laboratoire de Physique et Chimie des Nano Objets, LPCNO, UMR5215 INSA-UPS-CNRS, Institut National des Sciences Appliquées, 135 Avenue de Rangueil, 31077 Toulouse, France

<sup>b</sup>CNRS, LCC (Laboratoire de Chimie de Coordination) 205 Route de Narbonne, BP44099, F-31077 Toulouse Cedex 04, France; Université de Toulouse, UPS, INPT, F-31077 Toulouse Cedex 04, France

#### Contents

<b>1. General procedures.....</b>	<b>S2</b>
<b>2. Synthetic procedures.....</b>	<b>S4</b>
<b>3. Catalytic hydrogenation.....</b>	<b>S6</b>
<b>4. Wide-Angle X-ray Scattering (WAXS).....</b>	<b>S7</b>
<b>5. ATR FT-IR spectra.....</b>	<b>S8</b>
<b>6. TEM images.....</b>	<b>S13</b>
<b>7. HRTEM images.....</b>	<b>S16</b>
<b>8. NMR spectra.....</b>	<b>S16</b>
<b>9. References.....</b>	<b>S29</b>

## 1. General procedures

All oxygen and moisture sensitive operations were carried out under an argon atmosphere using standard vacuum-line and Schlenk techniques. Solvents were purchased from Sigma-Aldrich as HPLC grade and dried by means of an MBraun MB SPS800 purification system. Bis(1,5-cyclooctadiene)di- $\mu$ -methoxydiiridium(I), chlorodicyclohexylphosphine 97%, chloro(*tert*-butyl)phenylphosphine, and diphenylphosphine oxide 97% (**L2**) were purchased from Sigma-Aldrich. THF- $d_8$  was dried by distillation over Na/benzophenone under Ar and degassed by three freeze, pump, and thaw cycles. Chemical shifts of  $^1\text{H}$ ,  $^{13}\text{C}$  and  $^{31}\text{P}$ -NMR are reported in ppm, the solvent was used as internal standard. Signals are quoted as s (singlet), d (doublet), m (multiplet), br (broad), dd (double doublet), dt (double triplet), ddd (double doublet of doublets), dtd (double triplet of doublets), dm (double multiplet). Elemental analyses were performed by Kolbe (Mülheim, Germany).

### Transmission Electron Microscopy (TEM)

TEM analyses were performed at the “Toulouse characterization platform UMS-Castaing” on a JEOL JEM 1400 CX-T electron microscope operating at 120 kV. TEM grids were prepared by drop-casting of the crude colloidal solution in THF on a holey carbon-coated copper grid. Size histograms have been built with the help of the software ImageJ.

### High Resolution Transmission Electron Microscopy (HRTEM)

HRTEM observations were performed at the “Toulouse characterization platform UMS-Castaing” on a JEOL JEM 2010 electron microscope working at 200 kV with a resolution point of 2.35 Å. FFT treatments have been carried out with Digital Micrograph Version 3.7.4. TEM grids were prepared by drop-casting of the crude colloidal solution in THF on a holey carbon-coated copper grid.

### Energy Dispersive X-ray Spectroscopy (EDX)

EDX analyses were performed “Toulouse characterization platform UMS-Castaing” on a JEOL JEM 2010 electron microscope working at 200 kV with a resolution point of 2.35 Å. TEM grids were prepared by drop-casting of the crude colloidal solution in THF on a holey carbon-coated copper grid.

### **Wide-Angle X-ray Scattering (WAXS)**

WAXS analyses were performed at CEMES-CNRS. Samples were sealed in 1.5 mm diameter Lindemann glass capillaries. The samples were irradiated with graphite monochromatized molybdenum  $K_{\alpha}$  (0.071069 nm) radiation and the X-ray intensity scattered measurements were performed using a dedicated two-axis diffractometer. Radial distribution functions (RDF) were obtained after Fourier transformation of the reduced intensity functions.

### **Fourier Transform Infrared Spectroscopy (FT-IR)**

FT-IR measurements were carried out at the LPCNO on a Thermo Scientific Nicolet 6700 spectrometer in the range 4000–600  $\text{cm}^{-1}$ .

### **Nuclear Magnetic Resonance (NMR)**

$^1\text{H}$ ,  $^{13}\text{C}$  and  $^{31}\text{P}$  spectra were recorded at the LCC-Toulouse on Bruker Avance 400 and 300 spectrometers.

### **Magic Angle Spinning Solid State NMR (MAS-NMR)**

Solid-state NMR experiments were recorded at the LCC (Toulouse) on a Bruker Avance 400 spectrometer equipped with 3.2 mm probes. Samples were spun between 16 to 20 kHz at the magic angle using  $\text{ZrO}_2$  rotors.  $^{31}\text{P}$  MAS experiments were performed with Hahn-echo synchronized with the spinning rate (20 kHz) and a recycle delay of 20 s.  $^{31}\text{P}$  CP/MAS spectra were recorded with a recycle delay of 3 s and a contact time of 2 ms.  $^{31}\text{P}$  CPMG were acquired with 56 echoes, a delay between train of  $180^\circ$  pulse of 6 rotor periods and a recycle delay of 2s.  $^{31}\text{P}$  HETCOR-CPMG were recorded with 40 echoes, a delay between train of  $180^\circ$  pulse of 20 rotor periods, a recycle delay of 2s and a contact time of 0.3 ms.  $^{31}\text{P}$   $T_1$  were measured with saturation recovery method associated with Hahn-echo or CPMG schemes.

$^{13}\text{C}$  MAS experiments were performed with Hahn-echo synchronized with the spinning rate (18 kHz) and a recycle delay of 100 s.  $^{13}\text{C}$  CP/MAS spectra were recorded with a recycle delay of 3 s and a contact time of 2 ms. The  $^{13}\text{C}$  CP kinetics were obtained by varying the contact time between 0.5 ms to 30 ms.  $^{13}\text{C}$   $T_1^C$  and  $T_{1\rho}^C$  were measured with the Bruker pulse program cpxT1 and cpxT1rho. For the CP

kinetics and the  $T_1^C$  and  $T_{1\rho}^C$  measurements, the  $^{13}\text{C}$  spectra were first deconvoluted with the Dmfit software.<sup>1</sup> The CO area evolutions were then fitted with the GOSA-fit software.<sup>2</sup>

All the  $^{31}\text{P}$  and  $^{13}\text{C}$  spectra were recorded under high-power proton decoupling conditions. Chemical shifts for  $^1\text{H}$  and  $^{13}\text{C}$  are relative to TMS.  $^{31}\text{P}$  chemical shifts were referenced to an external 85%  $\text{H}_3\text{PO}_4$  sample.

## 2. Synthetic procedures

### *tert*-Butyl(phenyl)phosphine oxide (L1)

A rapidly stirred solution of chloro(*tert*-butyl)phenylphosphine (200.6 mg, 1 mmol) in THF (5 mL) was treated with degassed water (*ca.* 0.5 mL) at room temperature and the progress of the reaction was followed by  $^{31}\text{P}\{^1\text{H}\}$  NMR (*ca.* 5 h, > 99 %, no solvent, 202 MHz). The solvent was removed completely and the residue left under vacuum overnight and then dried by azeotropic distillation with toluene (2 x 10 mL). The residue was washed with hexane (2 x 2 mL) and then dried under high vacuum giving the product as a free flowing white powder. Yield: 161 mg, 0.88 mmol, 88 %.

$^1\text{H}$  NMR (500 MHz,  $\text{CDCl}_3$ ):  $\delta$  7.71 – 7.61 (m, 2H,  $\underline{\text{H}}_{\text{Ar}}$ ), 7.57 – 7.63 (m, 1H,  $\underline{\text{H}}_{\text{Ar}}$ ), 7.51 – 7.40 (m, 2H,  $\underline{\text{H}}_{\text{Ar}}$ ), 7.01 (d,  $^1J_{\text{HP}} = 453.1$  Hz, 1H), 1.14 (d,  $^3J_{\text{PH}} = 16.6$  Hz, 9H,  $\text{C}(\underline{\text{CH}}_3)_3$ ).

$^{31}\text{P}\{^1\text{H}\}$  NMR (202 MHz,  $\text{CDCl}_3$ ):  $\delta$  50.33 (s).

$^1\text{H}$ ,  $^{31}\text{P}$ ,  $^{31}\text{P}\{^1\text{H}\}$  and  $^{13}\text{C}\{^1\text{H}\}$  NMR data were consistent with those previously reported.<sup>3,4</sup>

### Dicyclohexylphosphine oxide (L3)

This substrate was prepared as described above for *tert*-butyl(phenyl)phosphine oxide (L1), starting from chlorodicyclohexylphosphine (233 mg, 1 mmol). Yield: 185.2 mg, 0.86 mmol, 86 %.

$^1\text{H}$  NMR (500 MHz,  $\text{CDCl}_3$ ):  $\delta$  6.41 (dt,  $J_{\text{PH}} = 453.1$  Hz,  $J_{\text{HH}} = 3.4$  Hz, 1H, P–H), 2.06 – 1.68 (m, 12H,  $\text{H}_{\text{cyclo}}$ ), 1.57 – 1.40 (m, 4H,  $\text{H}_{\text{cyclo}}$ ), 1.38 – 1.19 (m, 6H,  $\text{H}_{\text{cyclo}}$ ).

$^{31}\text{P}\{^1\text{H}\}$  NMR (202 MHz,  $\text{CDCl}_3$ ):  $\delta$  52.72 (s).

$^1\text{H}$ ,  $^{31}\text{P}\{^1\text{H}\}$  and  $^{13}\text{C}\{^1\text{H}\}$  NMR data were consistent with those previously reported.<sup>3,5</sup>

### Synthesis of stabilized Ir nanoparticles 1

Procedure analogous to that previously described for RuNPs.<sup>6</sup> **L1** (18.2 mg, 0.1 mmol) was dissolved in THF (10 mL), and the solution was transferred *via* cannula to a Fischer–Porter reactor containing a solution of bis(1,5-cyclooctadiene)di- $\mu$ -methoxydiiridium(I) (66.2 mg, 0.1 mmol) in THF (60 mL). The reactor was pressurized with 3 bar of  $\text{H}_2$  and vented twice. The reactor was then pressurized with 5 bar of  $\text{H}_2$  and the reaction mixture was vigorously stirred overnight at room temperature. The color of the solution turned from yellow to black. The hydrogen pressure was eliminated and the solvent was removed under vacuum. The IrNPs were precipitated and washed with methanol (2 x 40 mL) and dried under vacuum.

$^{31}\text{P}$  MAS NMR:  $\delta$  68 ppm.

Elemental analysis (%): Ir, 47.86; P, 4.17.

EDX (%): Ir, 45.72; P, 4.27.

### Synthesis of stabilized Ir nanoparticles 2

The nanoparticles **2** were prepared in an identical manner to **1** except **L2** (20.2 mg, 0.1 mmol) was used in place of **L1**.

$^{31}\text{P}$  MAS NMR:  $\delta$  29 ppm.

Elemental analysis (%): Ir, 50.44; P, 4.89.

### Synthesis of stabilized Ir nanoparticles **3**

The nanoparticles **3** were prepared in an identical manner to **1** except **L3** (21.4 mg, 0.1 mmol) was used in place of **L1**.

$^{31}\text{P}$  MAS NMR:  $\delta$  94 ppm.

Elemental analysis (%): Ir, 48.65; P, 4.69.

### 3. Catalytic hydrogenation

Catalytic experiments were performed in a HEL 24–multireactor (volume of the tubes 1.5 mL). In a typical experiment, 1 mg of IrNPs (0.0025 mmol of Ir assuming % of Ir from elemental analysis) in 0.75 mL of THF (as a standard solution, freshly prepared prior to use) was mixed with 1 mmol of substrate in 1.5 mL vials and the reactor was sealed under argon atmosphere in a glove box. The reactor was then pressurized with 5 bar of hydrogen and depressurized three times to purge and finally pressurized to the required pressure (10 or 20 bar). The reactor was stirred overnight at room temperature. After 18 h, the reactor was slowly depressurized and samples from each reaction were filtered through a silica plug and evaporated to dryness at 150 mbar using a rotary evaporator at room temperature. The residue was dissolved in  $\text{CDCl}_3$  and analyzed by  $^1\text{H}$  NMR to determine the conversion and selectivity.

#### 4. Wide-Angle X-ray Scattering (WAXS) spectra

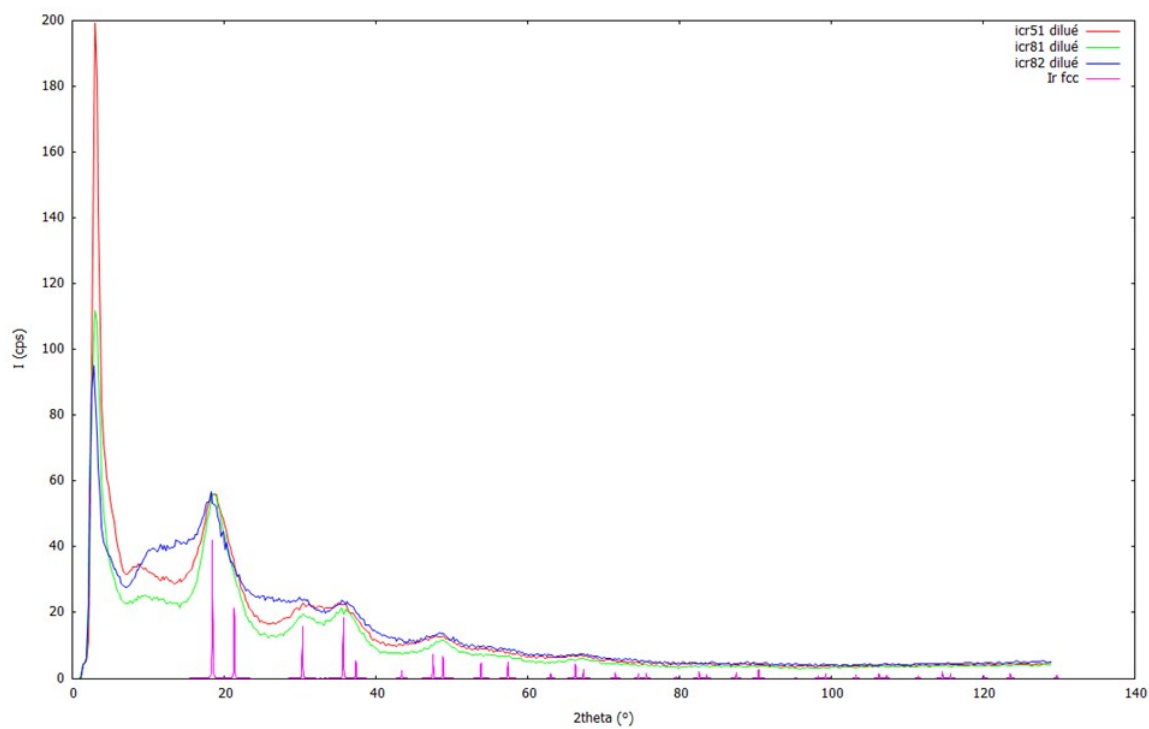


**Figure S1.** WAXS analysis of **1** (blue), **2** (green) and **3** (red).

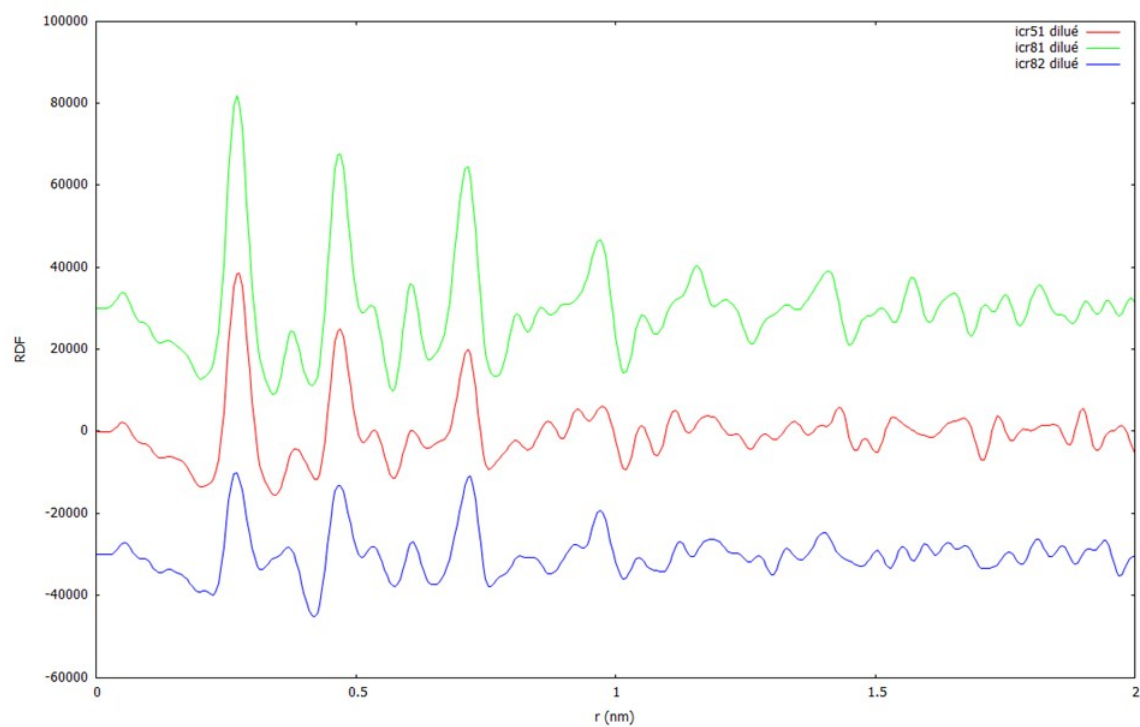


**Figure S2.** RDF analysis of **1** (blue), **2** (green) and **3** (red).

## 5. ATR FT-IR spectra

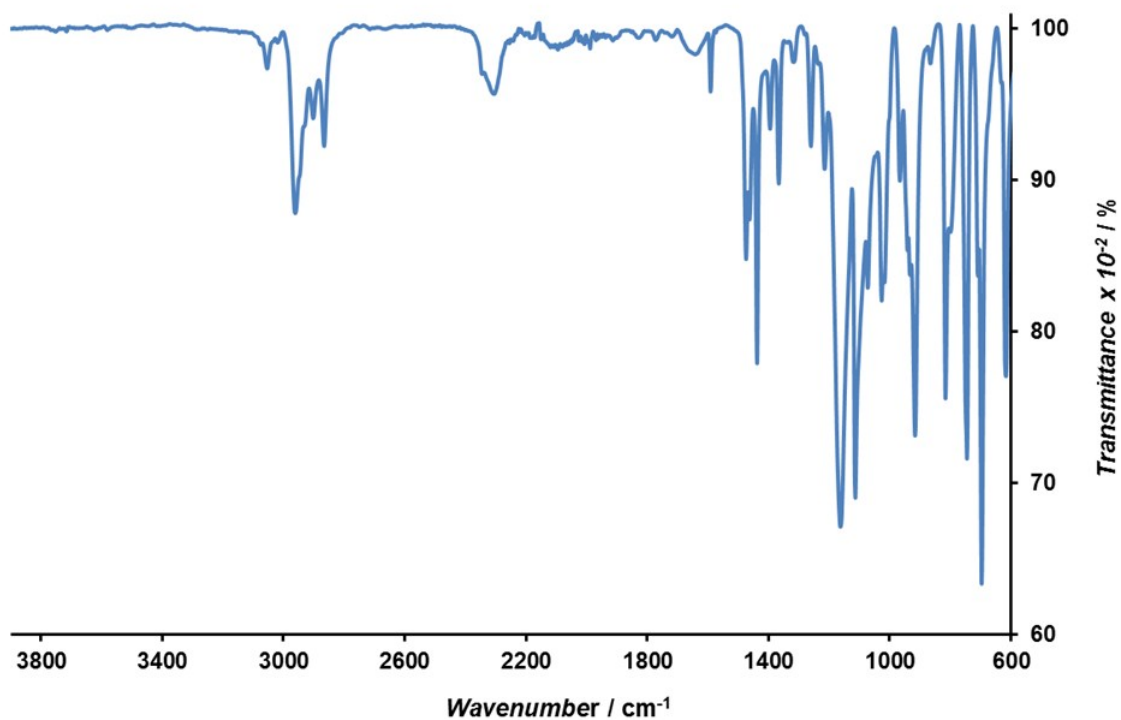


Figure S3. ATR FT-IR spectrum of L1.

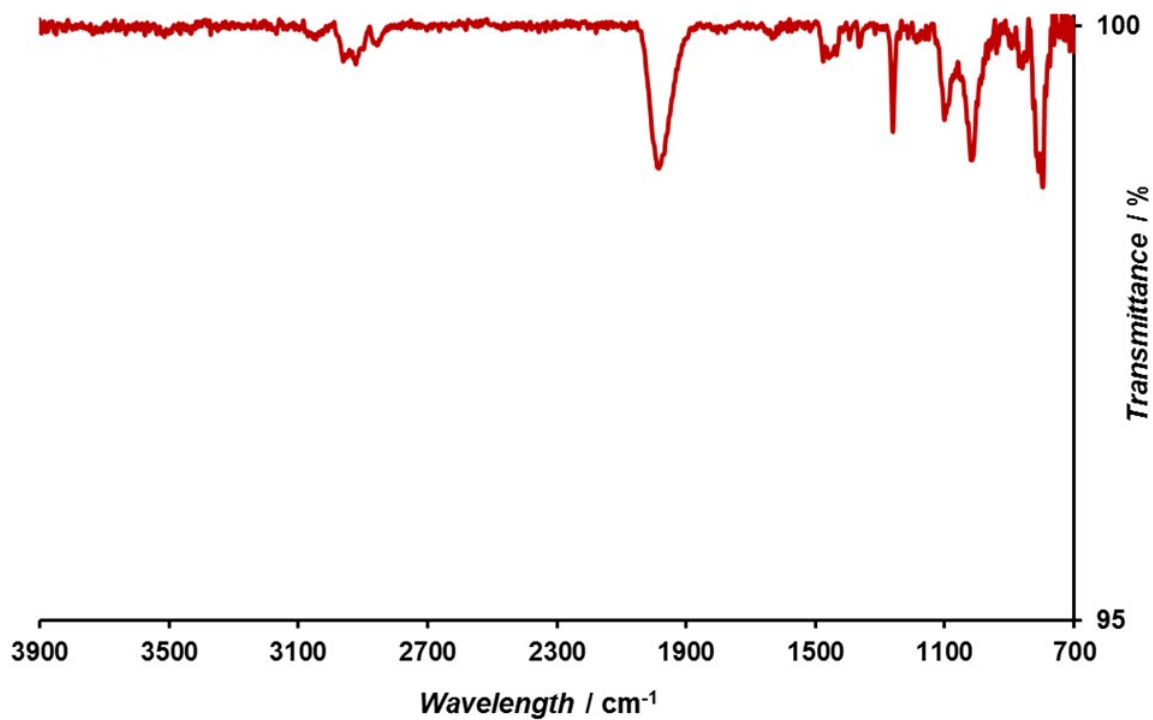


Figure S4. ATR FT-IR spectrum of 1.



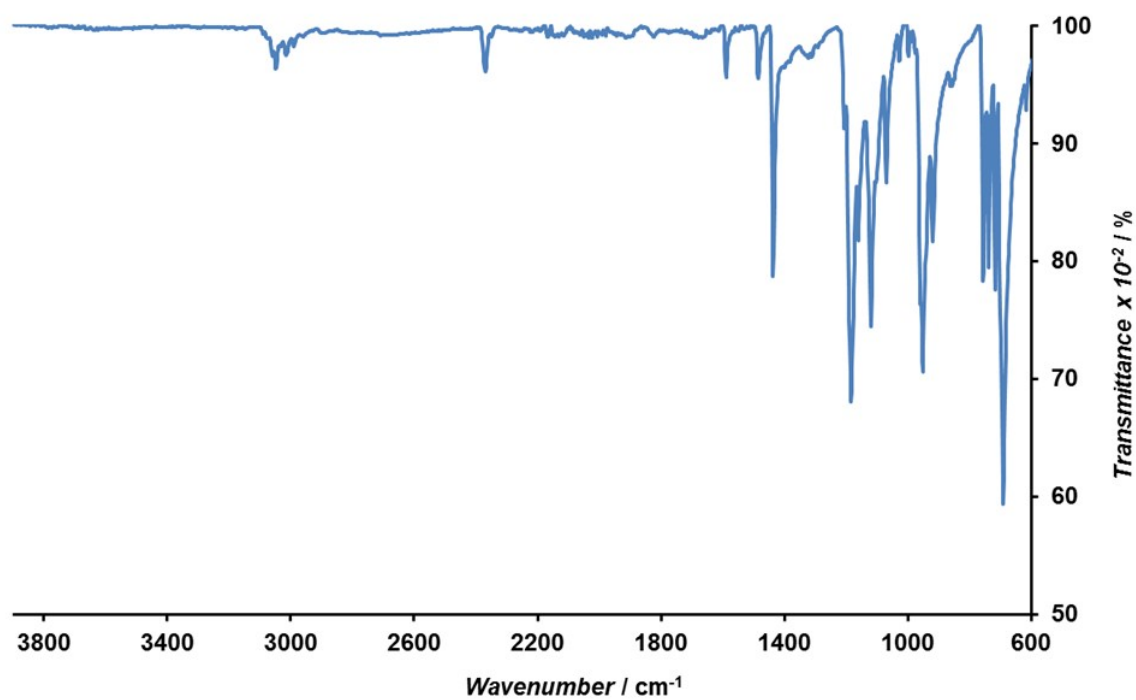


Figure S5. ATR FT-IR spectrum of L2.

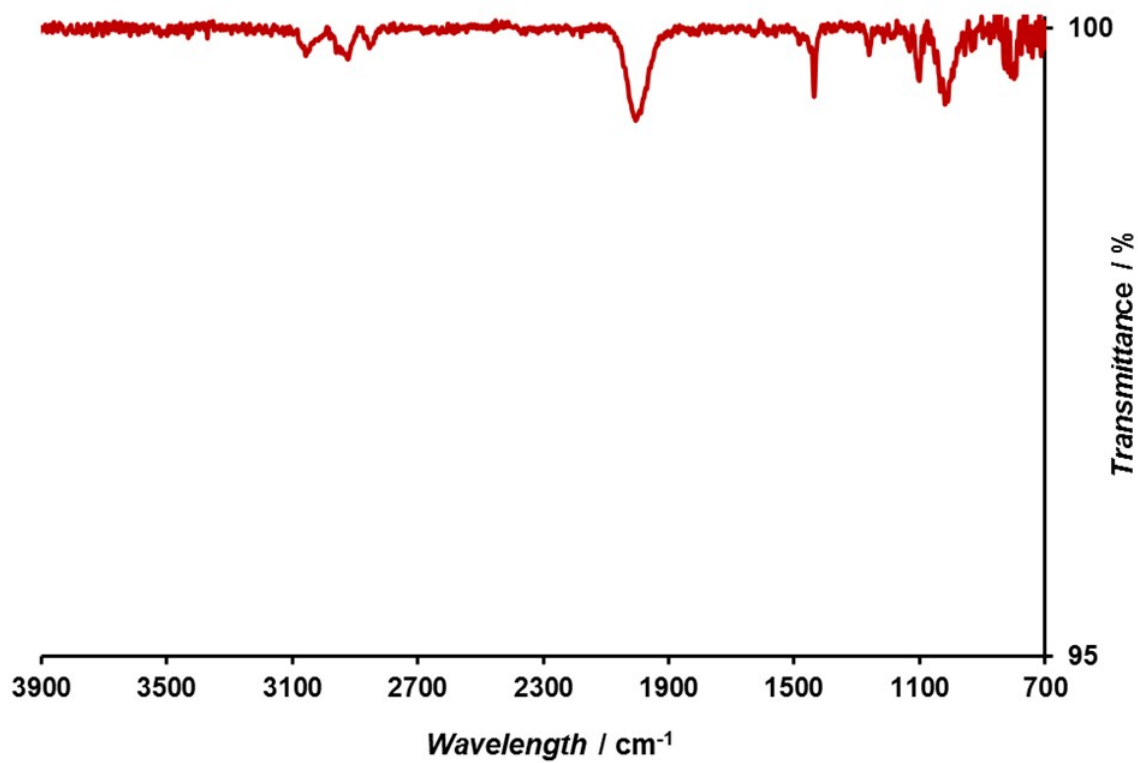
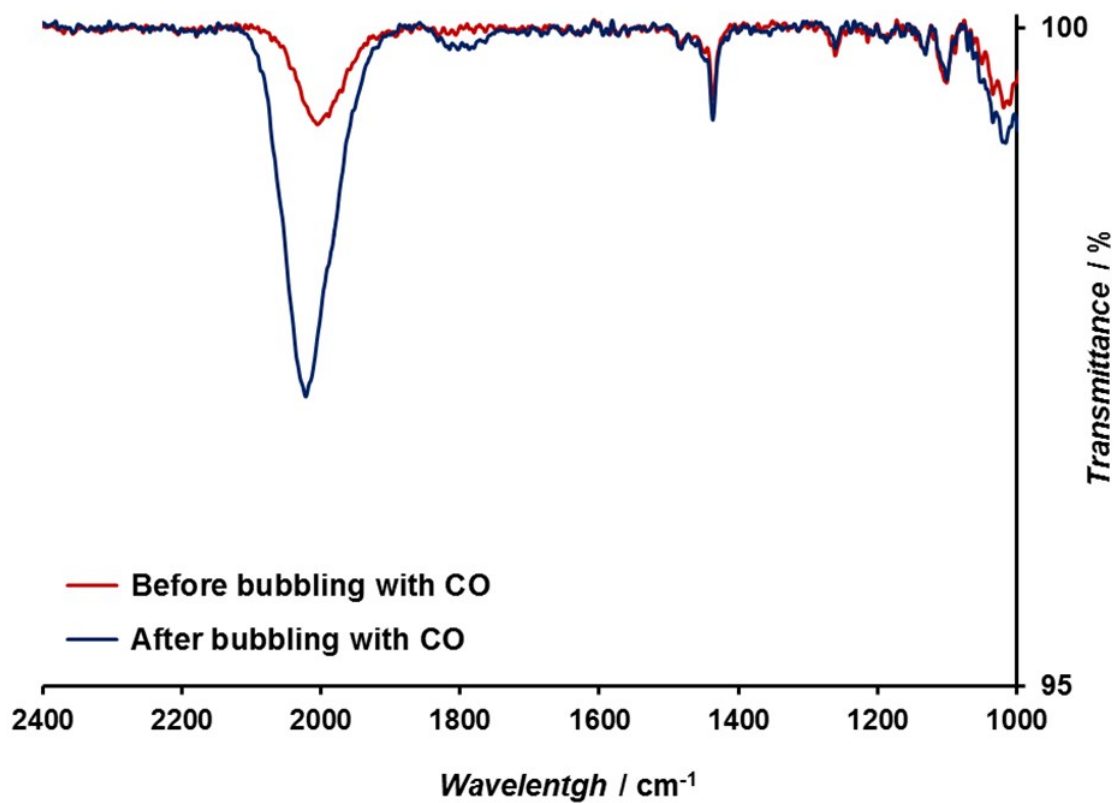
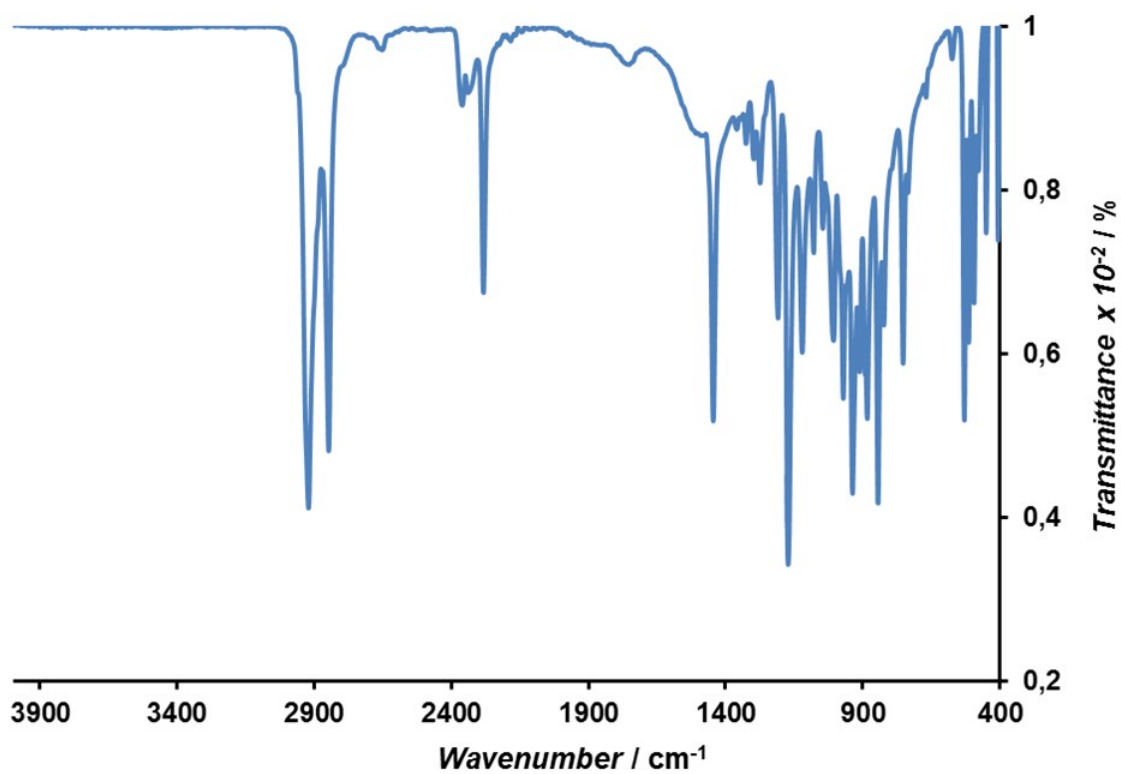


Figure S6. ATR FT-IR spectrum of 2.



**Figure S7.** Overlay of ATR-IR spectra of **2** before and after bubbling with CO in the region 1000–2400  $\text{cm}^{-1}$ .



**Figure S8.** ATR FT-IR spectrum of **L3**.

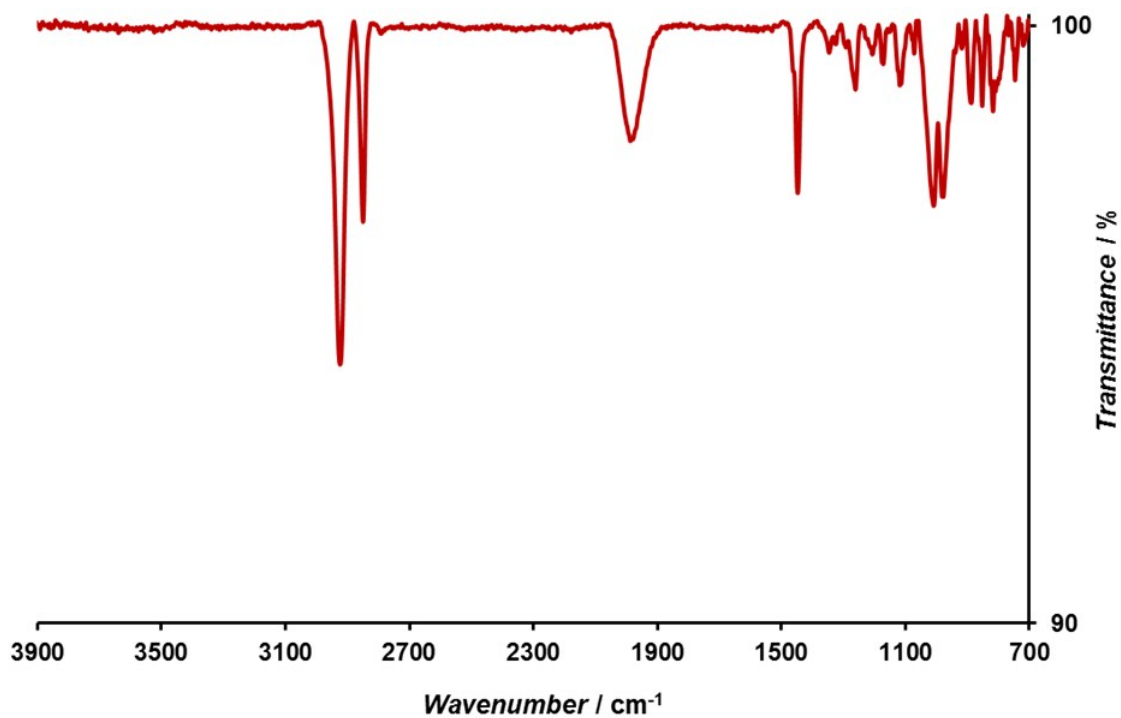


Figure S9. ATR FT-IR spectrum of **3**.

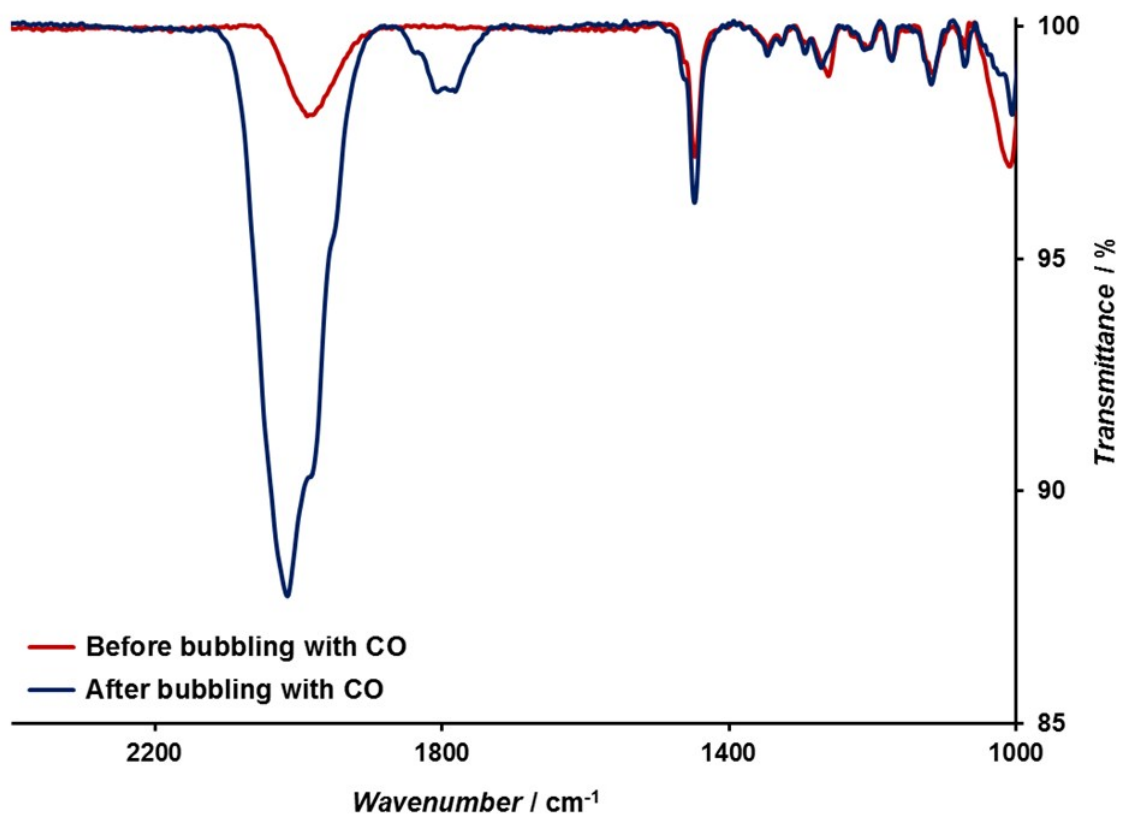
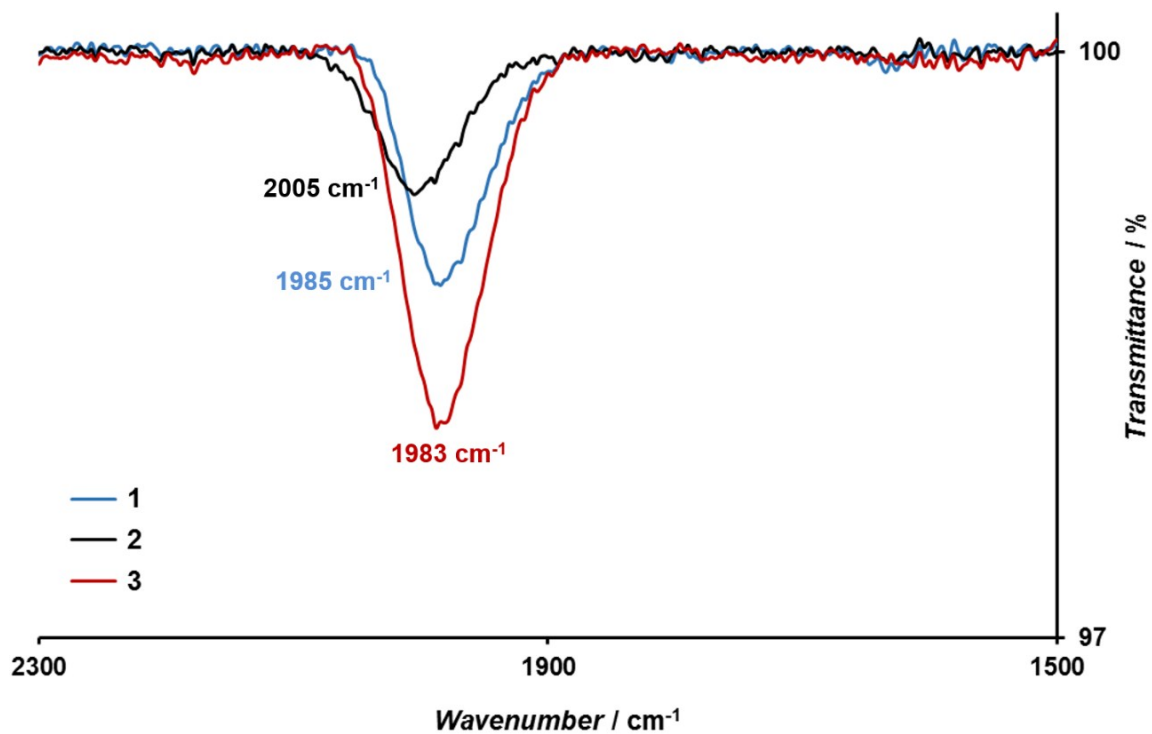
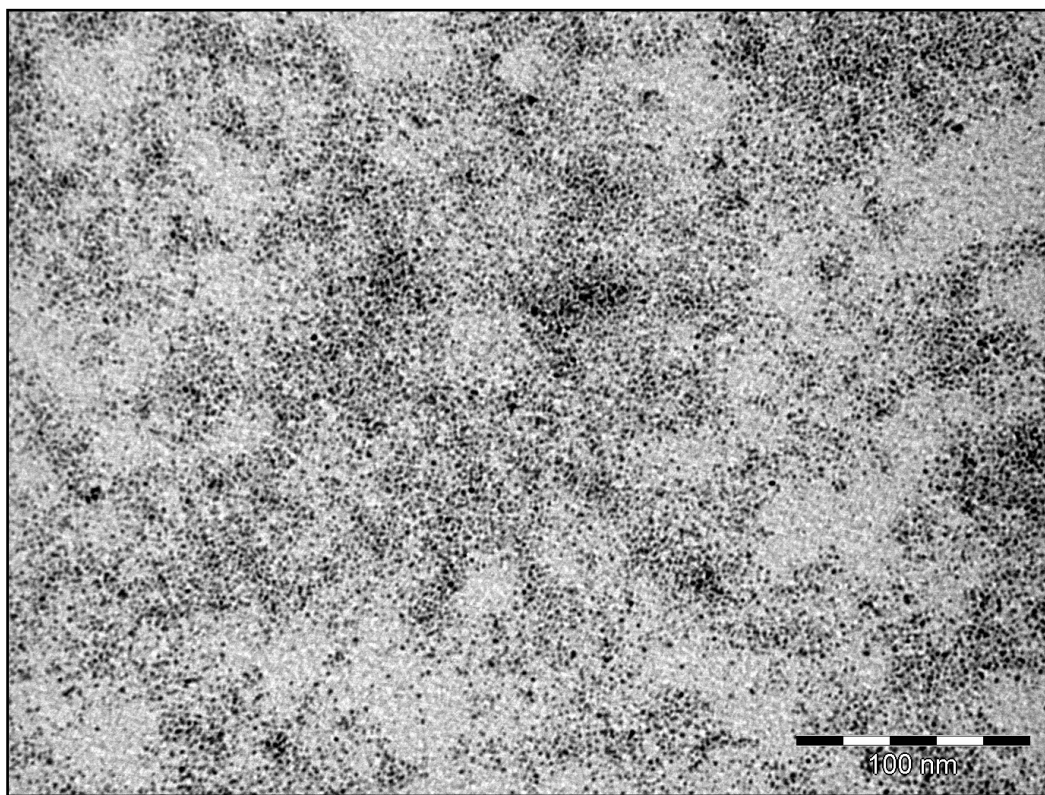
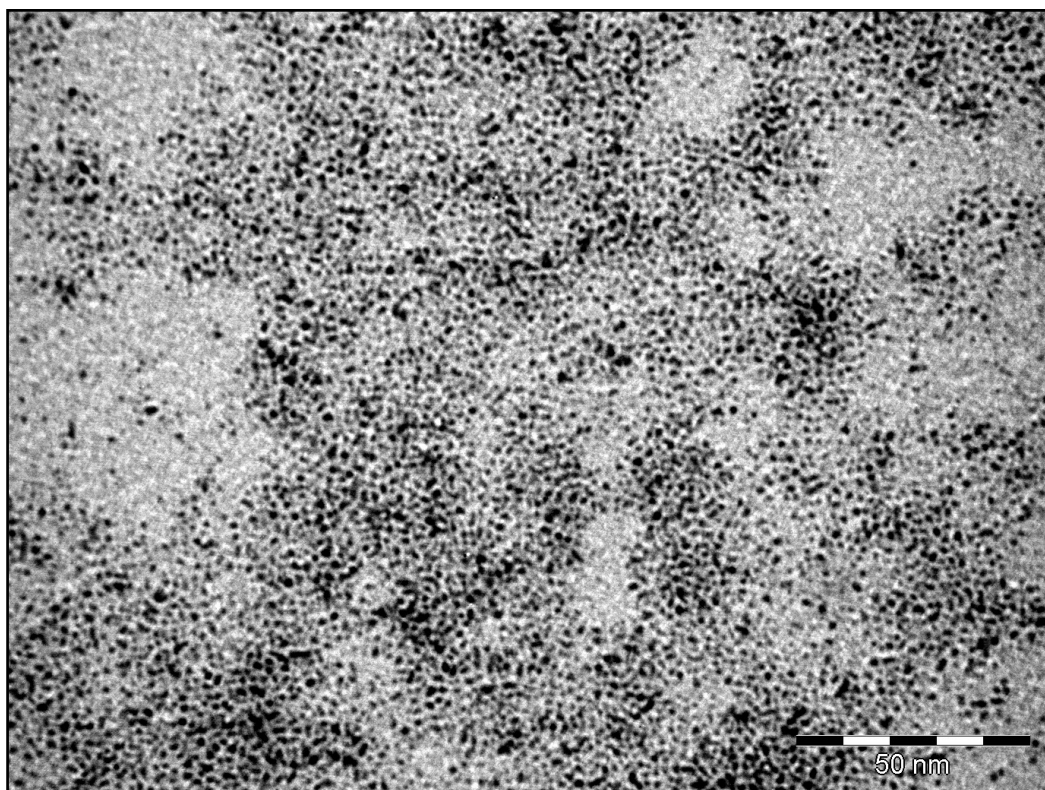


Figure S10. Overlay of ATR-IR spectra of **3** before and after bubbling with CO in the region 1000–2400  $\text{cm}^{-1}$

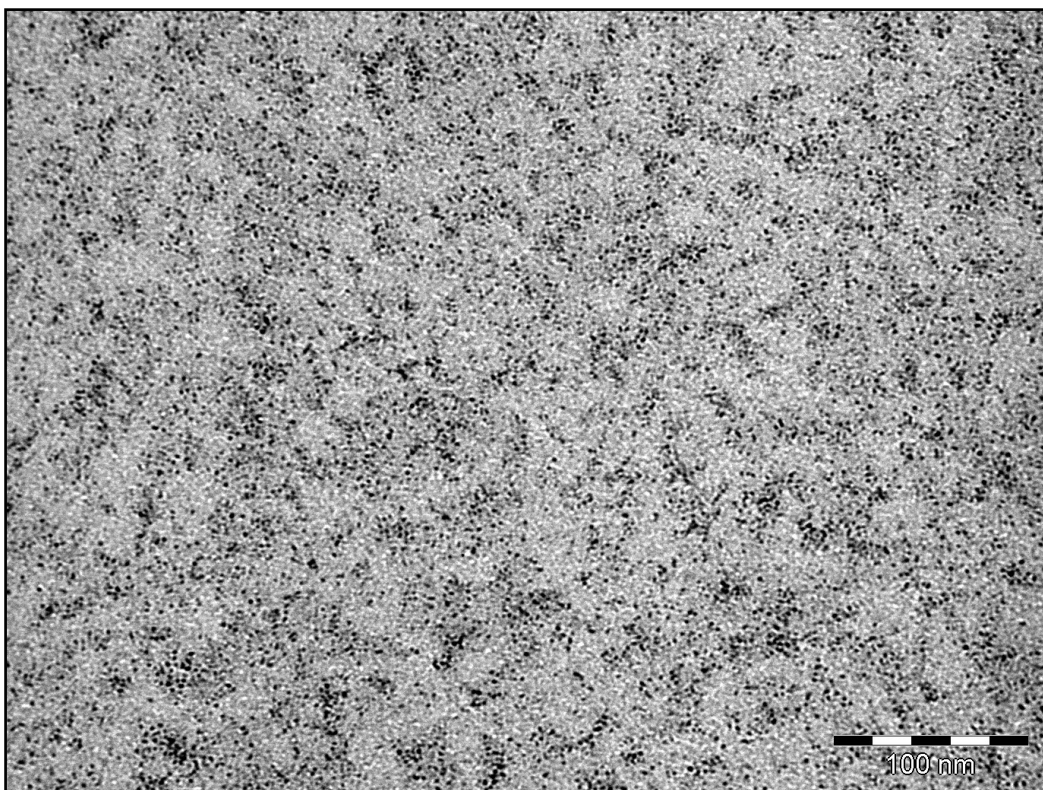
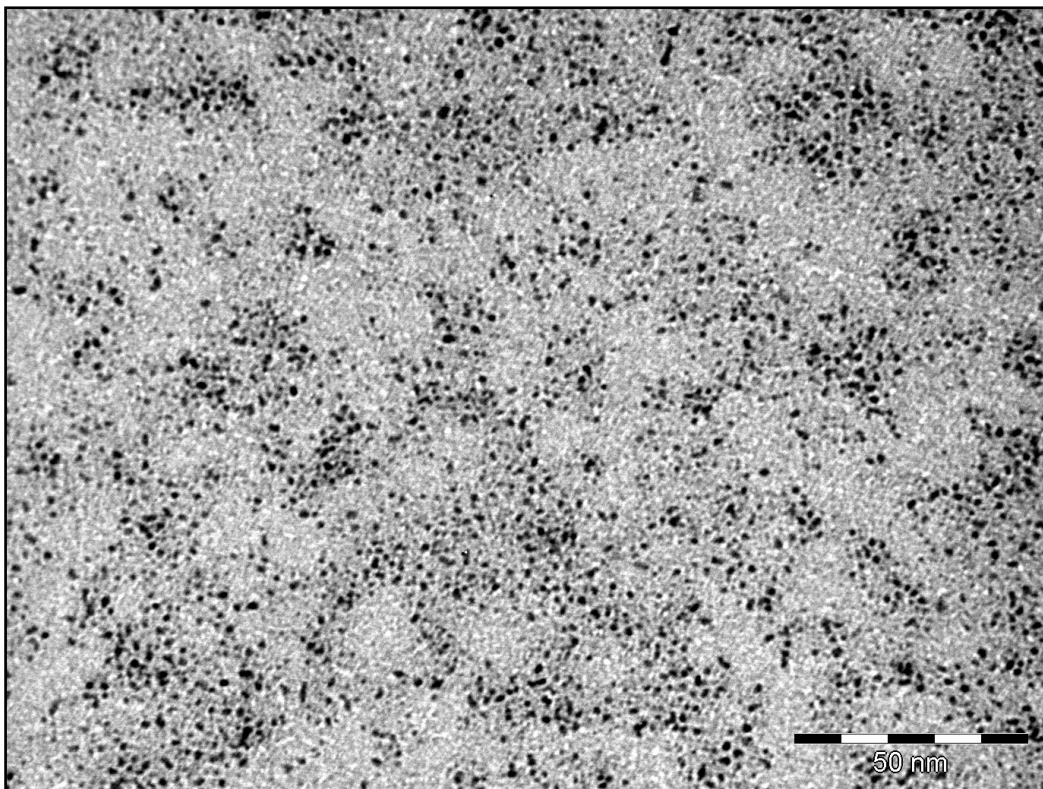


**Figure S11.** Overlay of ATR-IR spectra of **1** (blue), **2** (black) and **3** (red) before bubbling with CO in the region 1500–2300  $\text{cm}^{-1}$ .

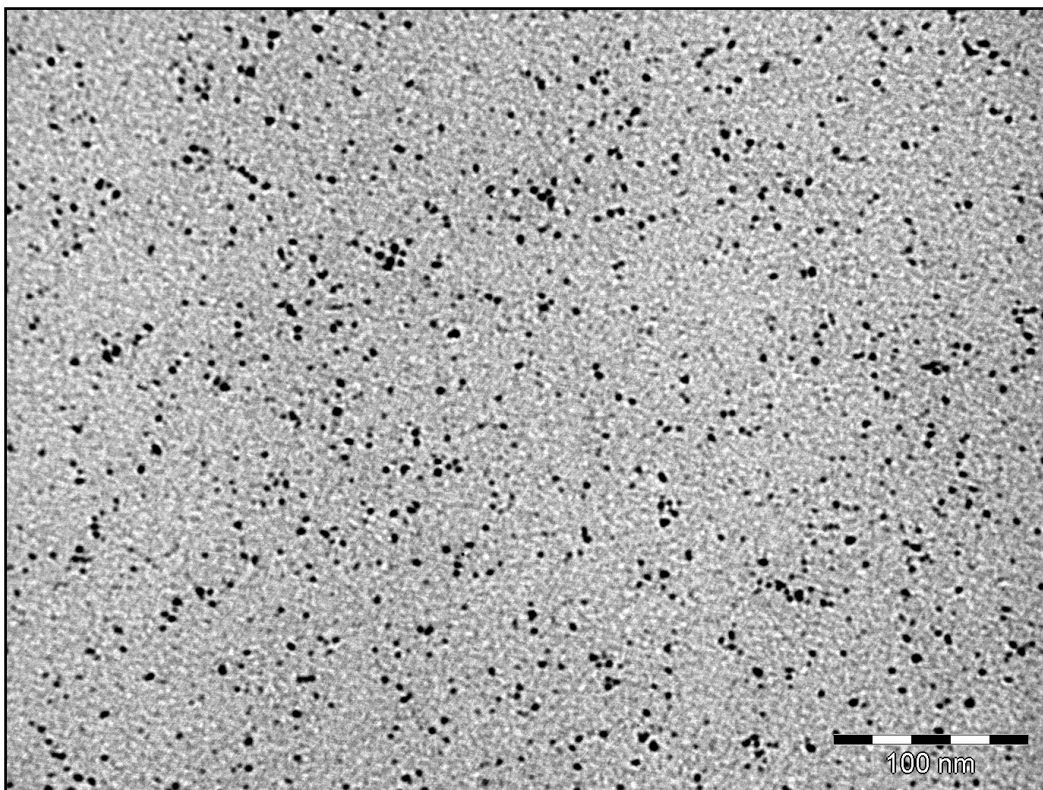
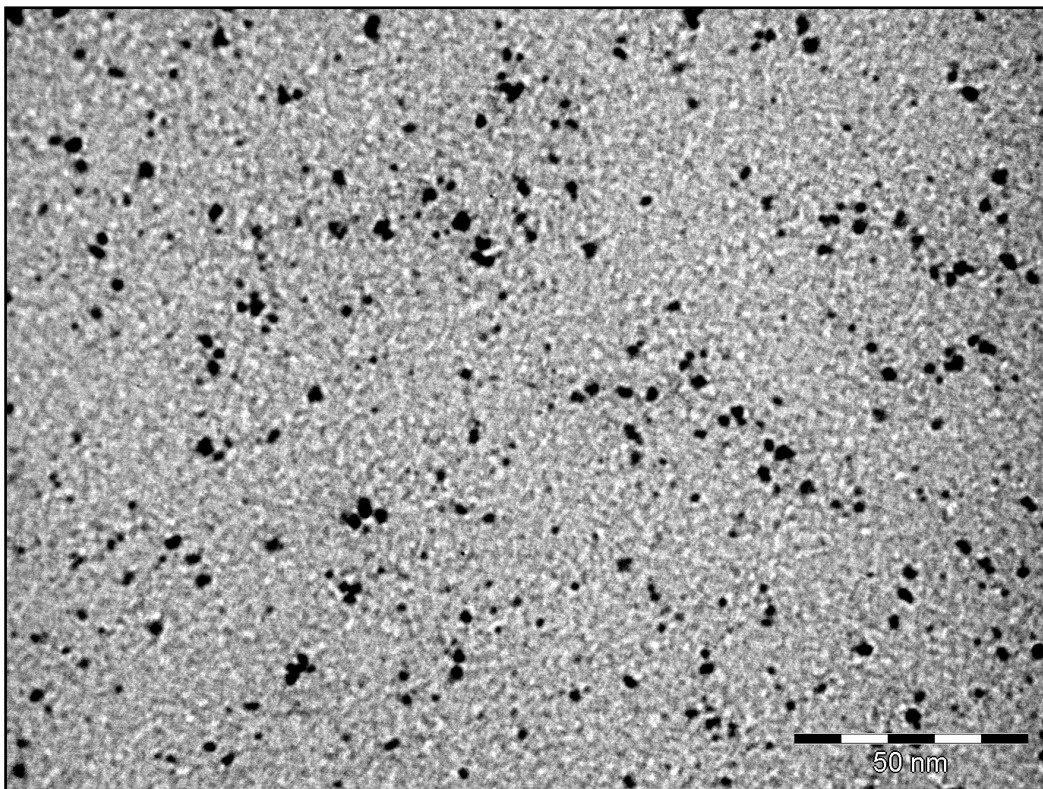
6. TEM images



Figures S12 and S13. Selected TEM images for 1.



**Figures S14 and S15.** Selected TEM images for **2**.



Figures S16 and S17. Selected TEM images for 3.

## 7. HRTEM images

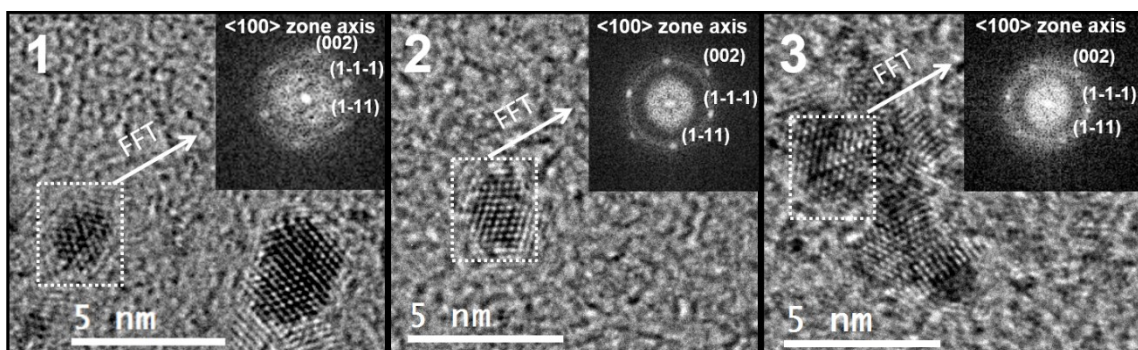


**Figure S18.** HRTEM micrographs and Fast Fourier Transform of a single particle for IrNPs 1–3.

## 8. NMR spectra

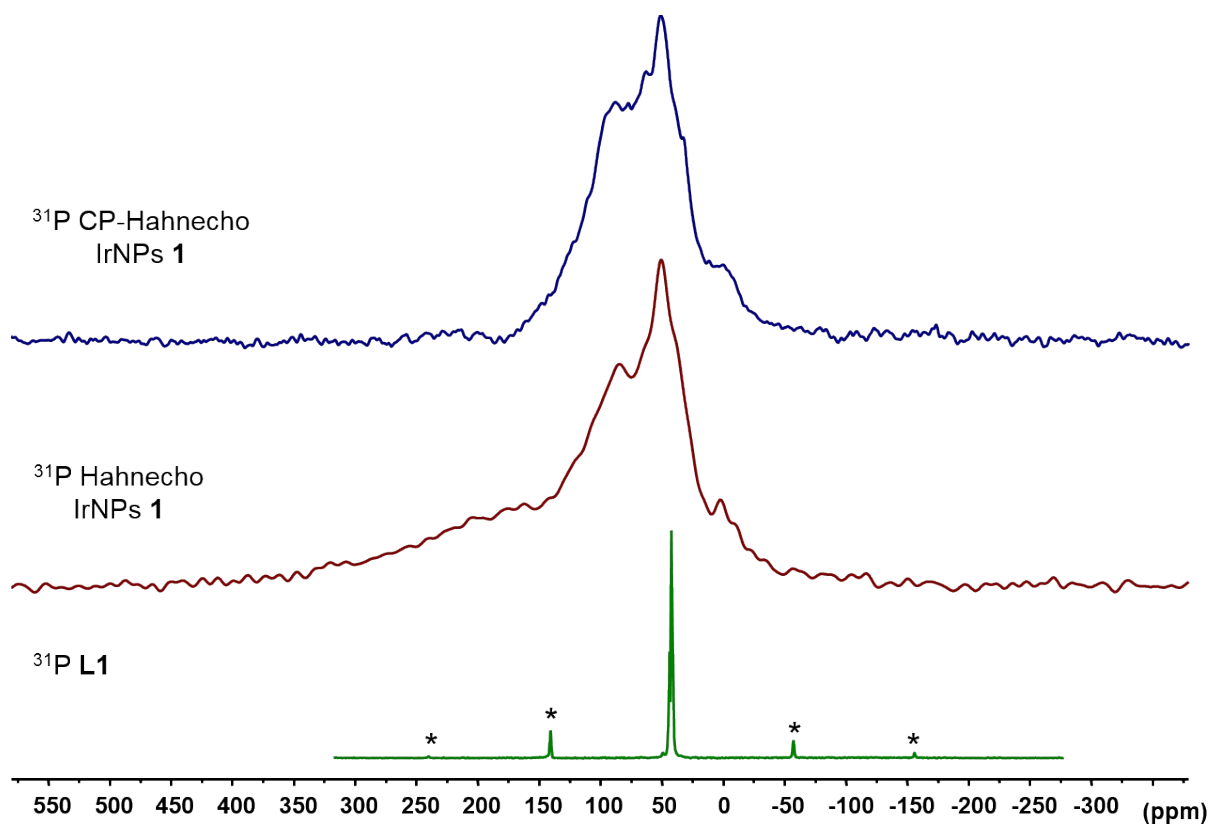


**Figure S19.**  $^{31}\text{P}$  Hahn-echo MAS NMR spectra of IrNPs 1 and L1. \* denote spinning side bands.



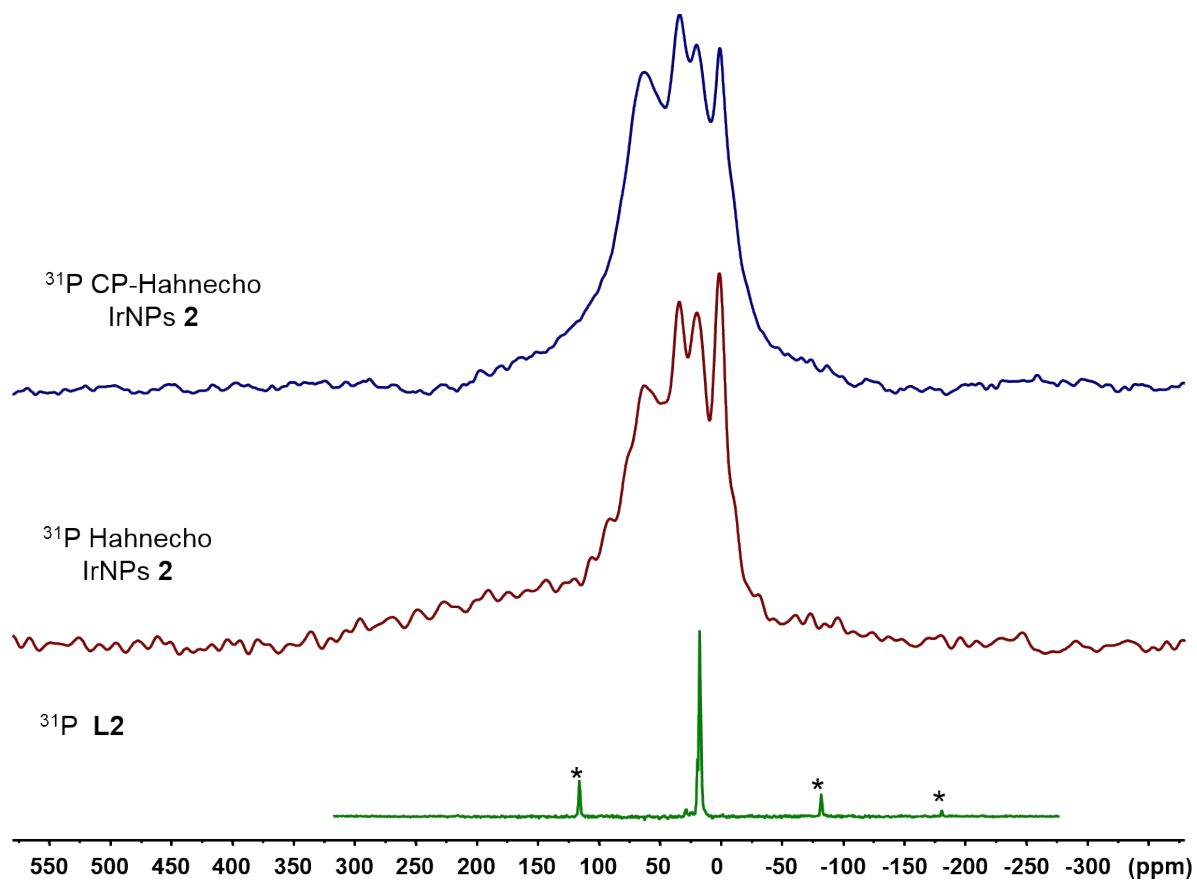


**Figure S20.**  $^{31}\text{P}$  Hahn-echo MAS NMR spectra of IrNPs 2 and L2. \* denote spinning side bands.

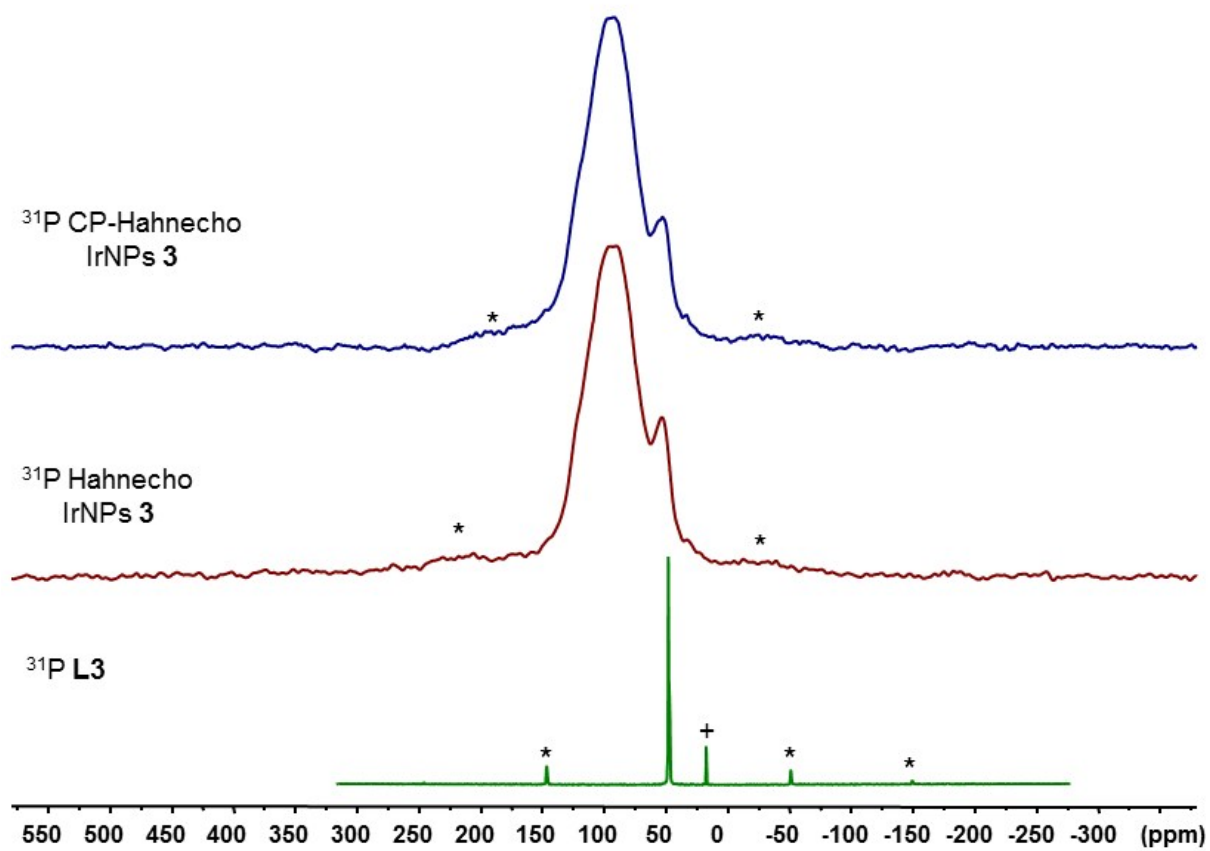


**Figure S21.**  $^{31}\text{P}$  Hahn-echo MAS NMR spectra of IrNPs **3** and **L3**. \* denote spinning side bands. + unknown impurity.

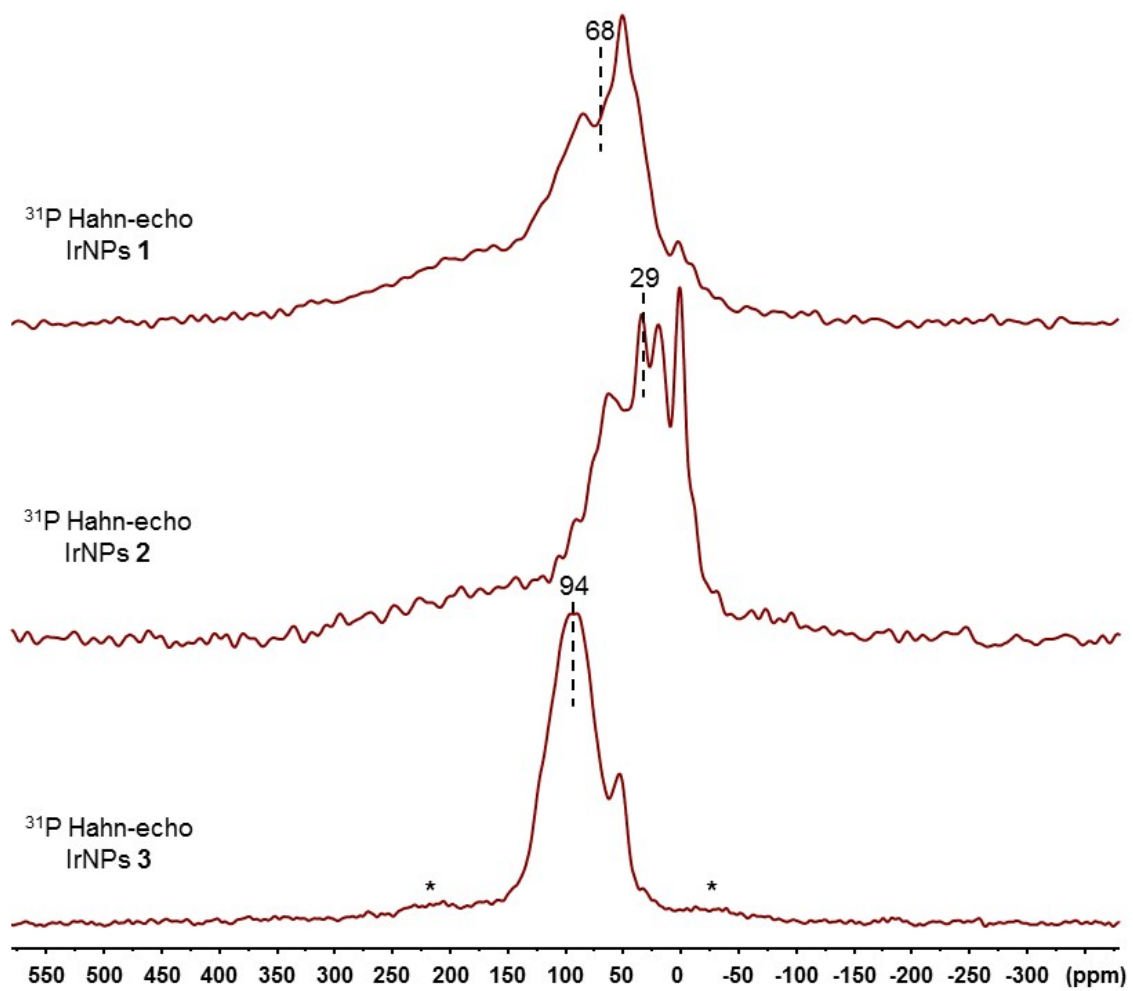


**Figure S22.**  $^{31}\text{P}$  Hahn-echo MAS NMR spectra of IrNPs 1–3. \* denote spinning side bands.

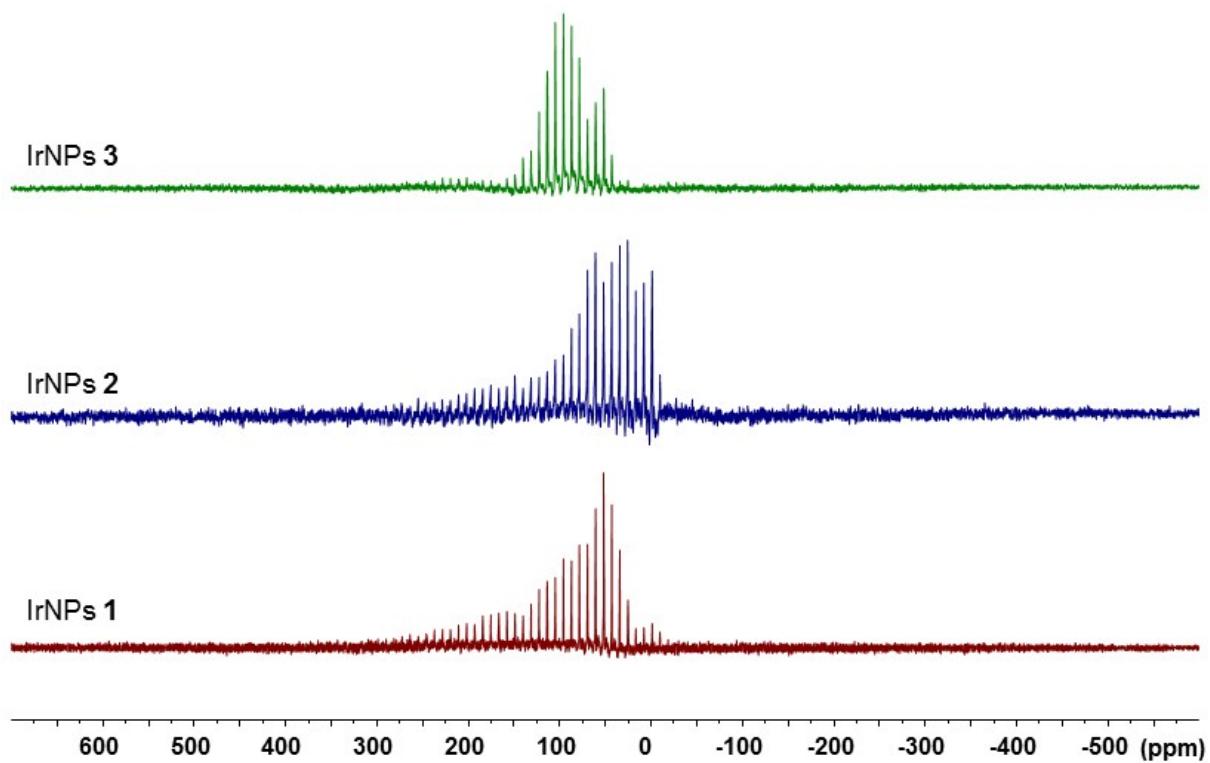


**Figure S23.**  $^{31}\text{P}$  MAS CPMG NMR spectra of IrNPs 1–3. The recovery time was fixed to a low value (2s) in order to emphasize the high frequency signal of Knight-shifted  $^{31}\text{P}$  resonances (see below).

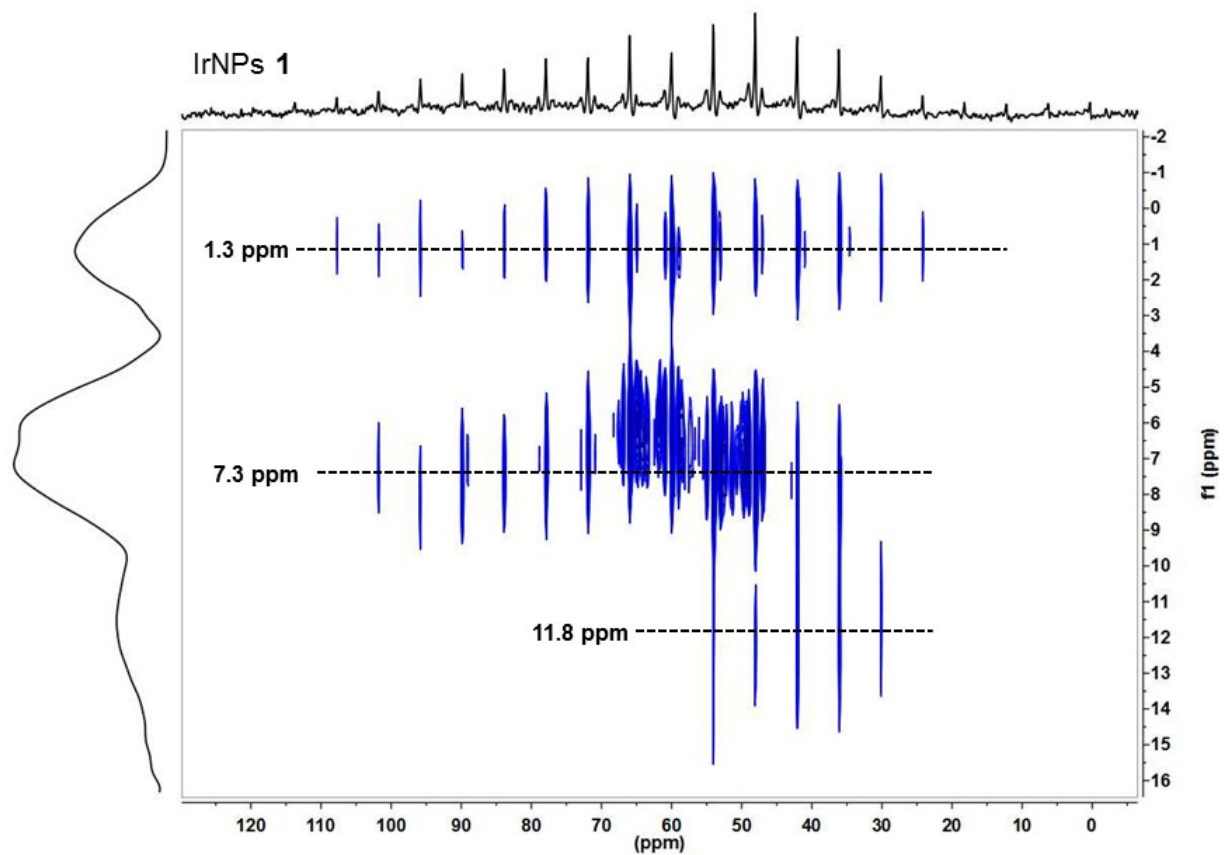


**Figure S24.**  $^{31}\text{P}$  CPMG-HETCOR MAS NMR spectrum of IrNPs **1**. Lines are given as guide to the eyes.

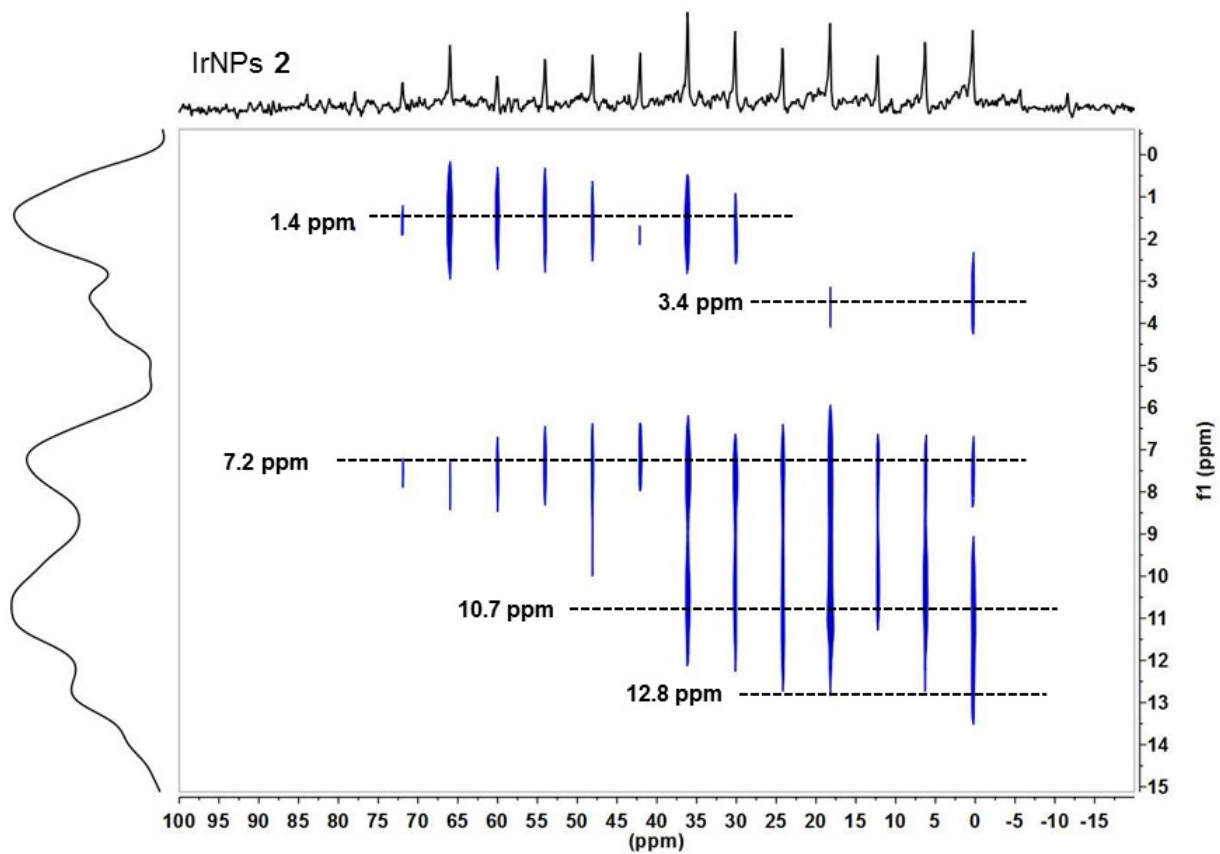


**Figure S25.**  $^{31}\text{P}$  CPMG-HETCOR MAS NMR spectrum of IrNPs **2**. Lines are given as guide to the eyes.

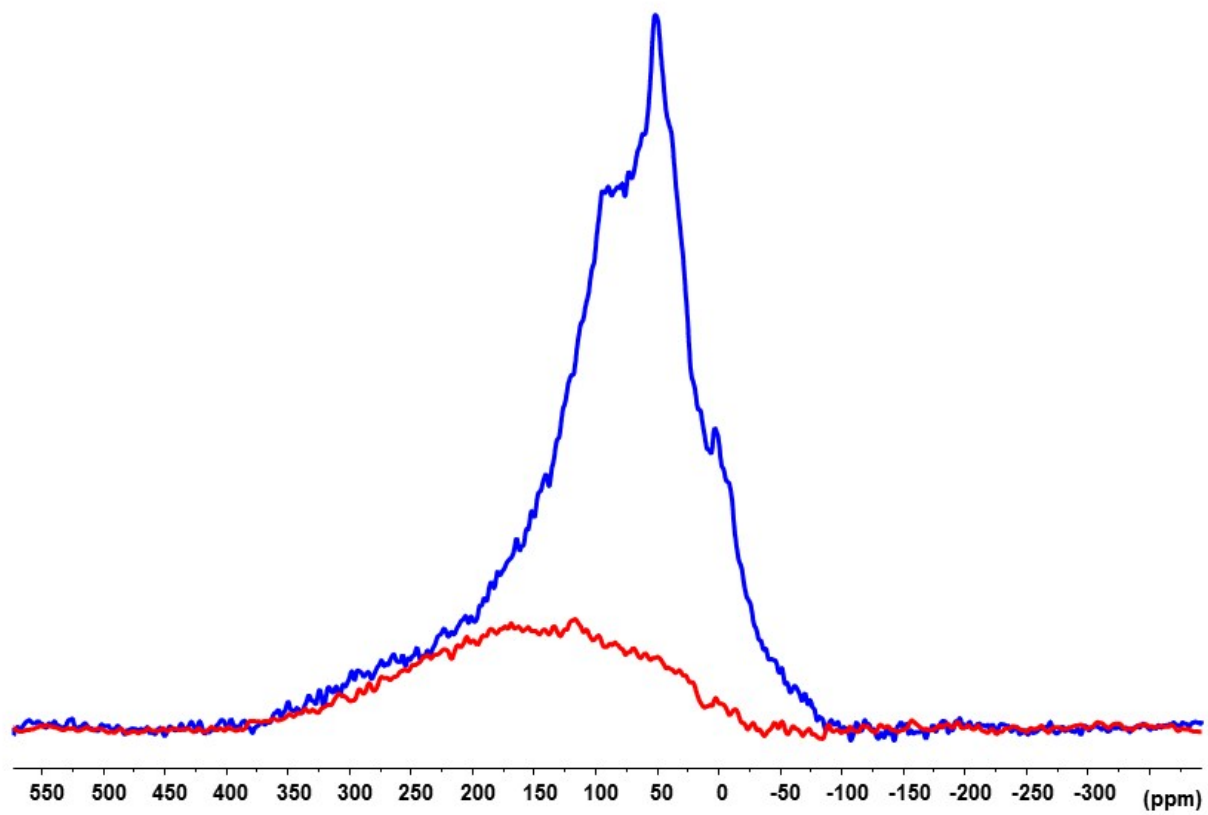


**Figure S26.**  $^{31}\text{P}$  Hahn-echo MAS NMR spectra of IrNPs **1** after saturation and recovery time of 100 ms (red) and 100s (blue).

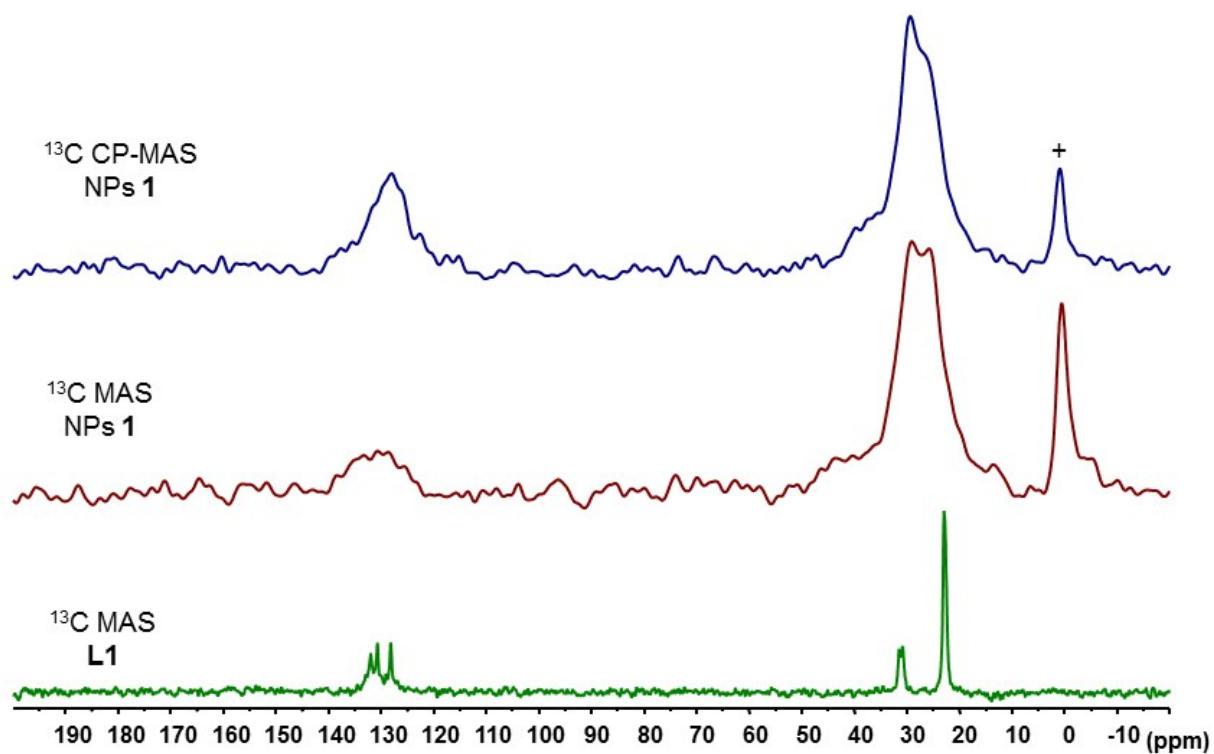


**Figure S27.**  $^{13}\text{C}$  MAS NMR spectra of IrNPs **1** and **L1**. + denotes grease.

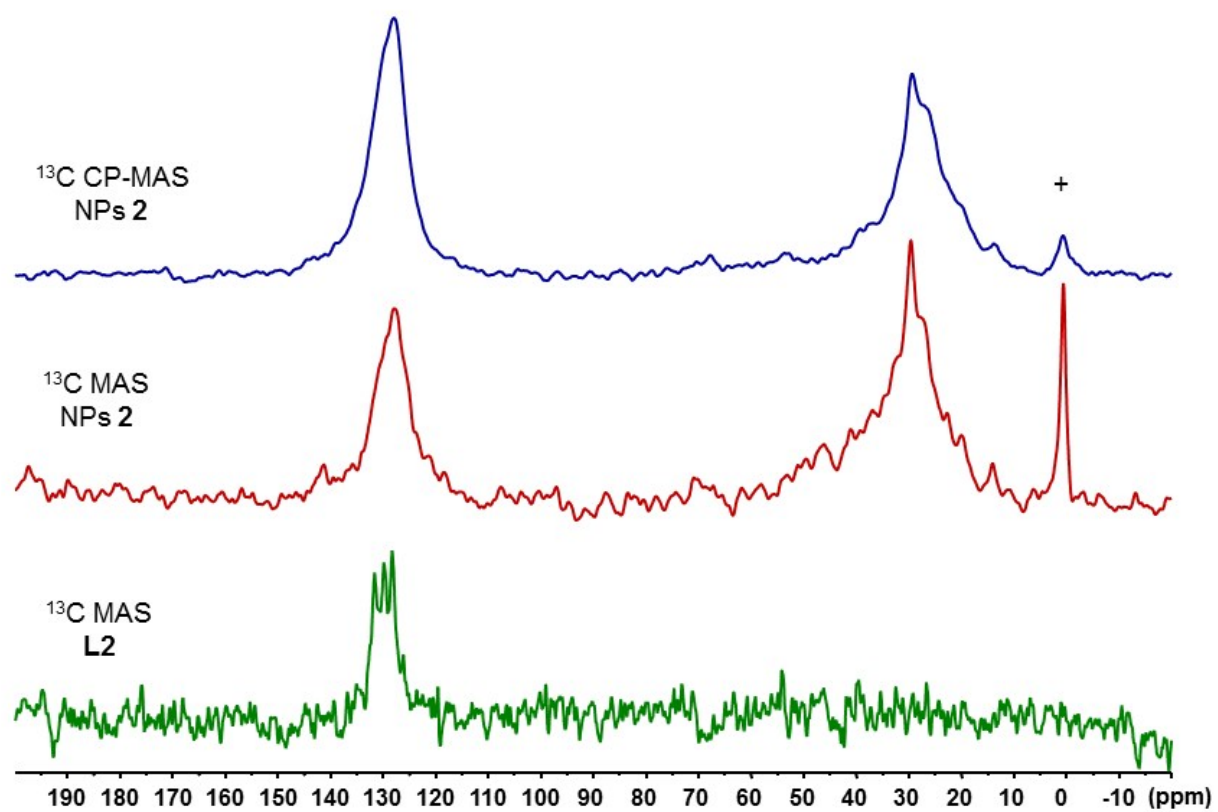


**Figure S28.**  $^{13}\text{C}$  MAS NMR spectra of IrNPs **2** and **L2**. + denotes grease.



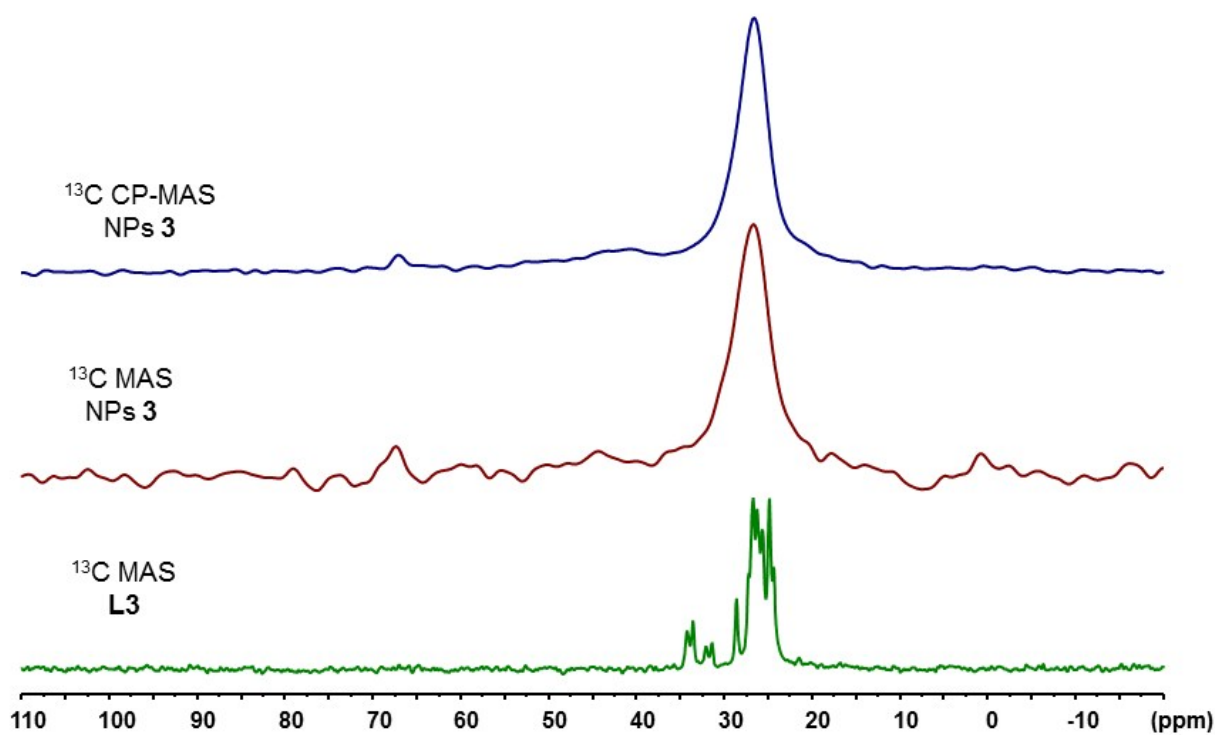


**Figure S29.**  $^{13}\text{C}$  MAS NMR spectra of IrNPs 3 and L3.

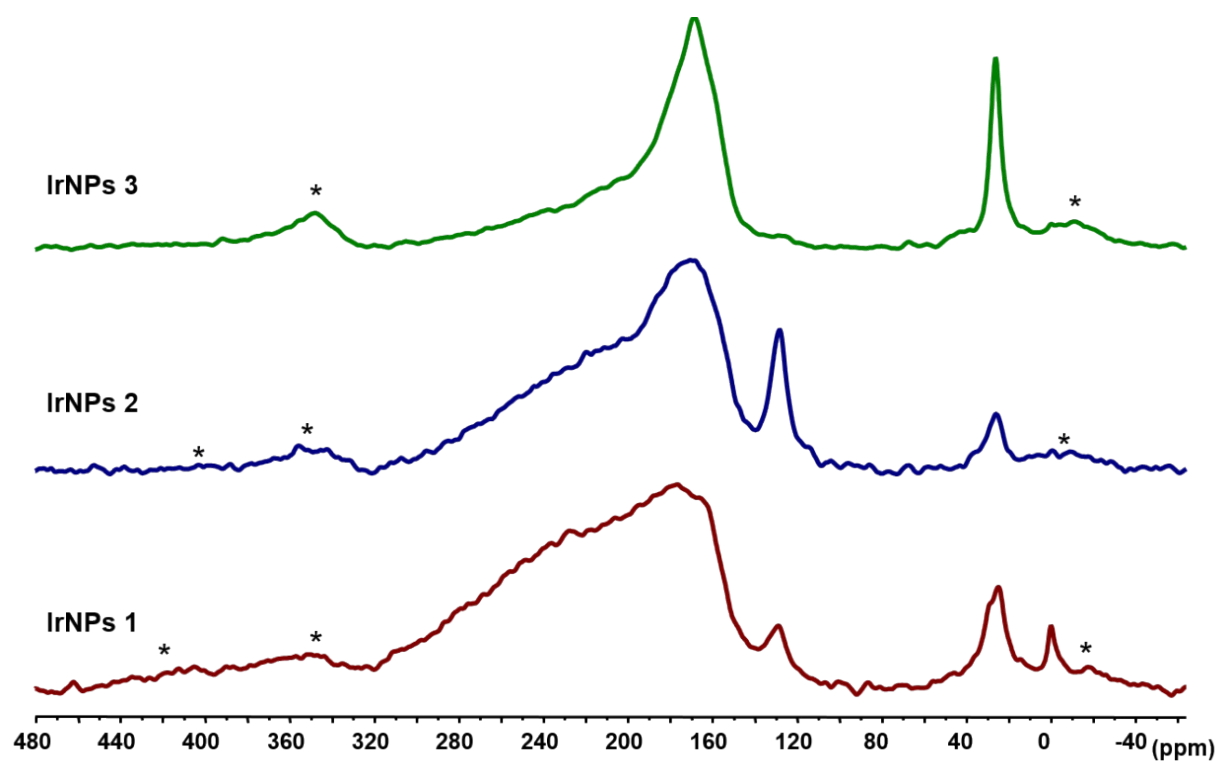


**Figure S30.**  $^{13}\text{C}$  Hahn-echo MAS NMR spectra (recovery time 100s) of 1–3 after exposure to  $^{13}\text{CO}$  (1 bar; R.T.; 20 h). \* denote spinning side bands.

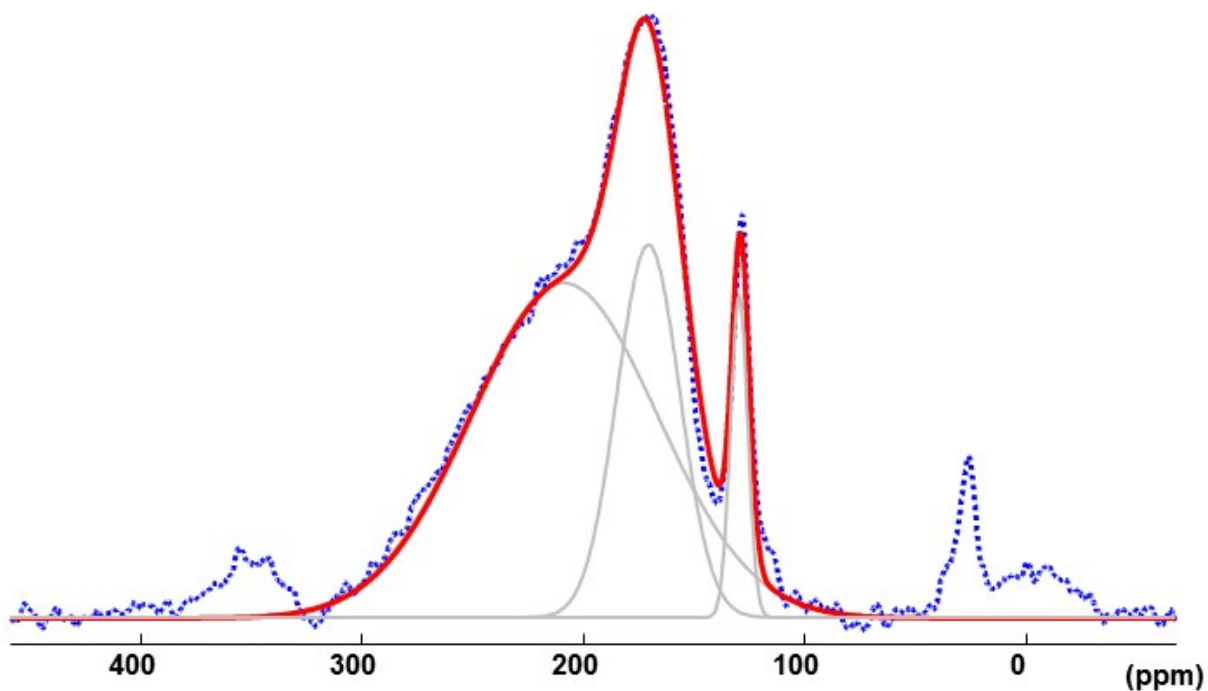


**Figure S31.** Example of CO signal deconvolution.  $^{13}\text{C}$  Hahn-echo MAS NMR spectrum of IrNPs **2** (dotted line, blue) compared to simulated spectrum (in red).

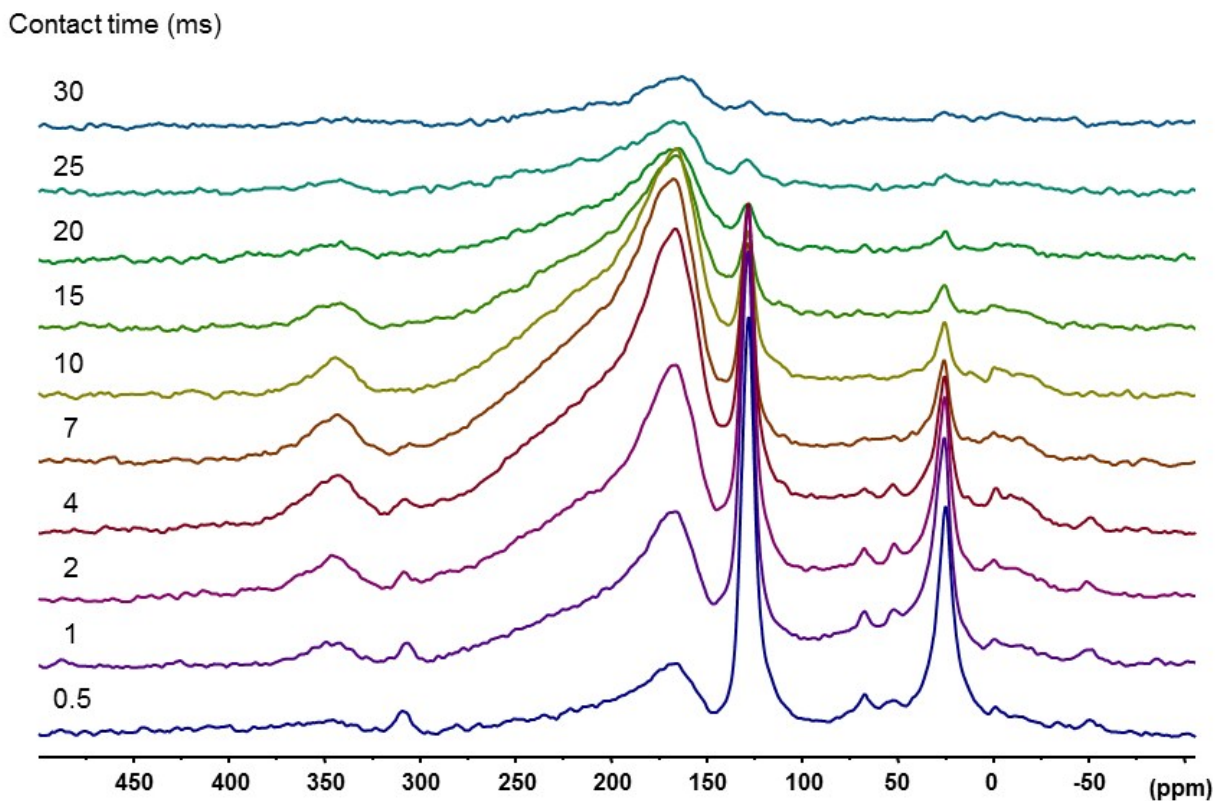
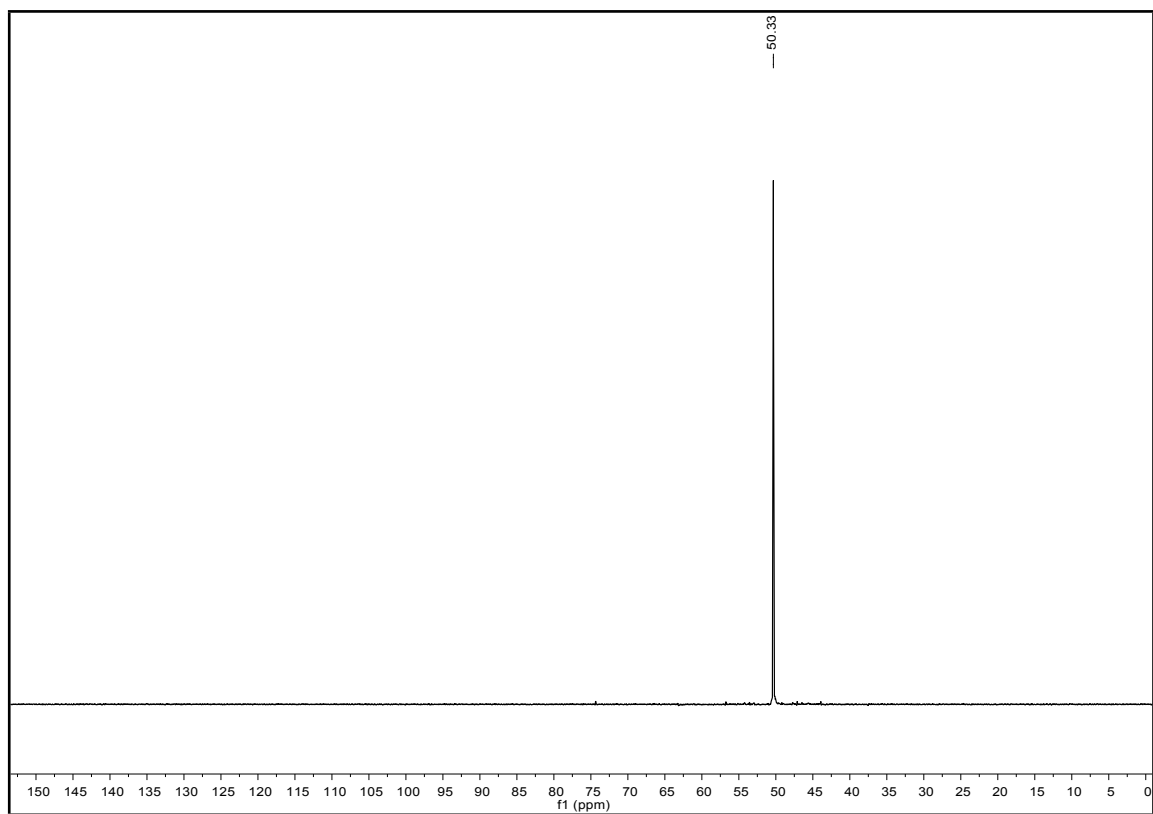
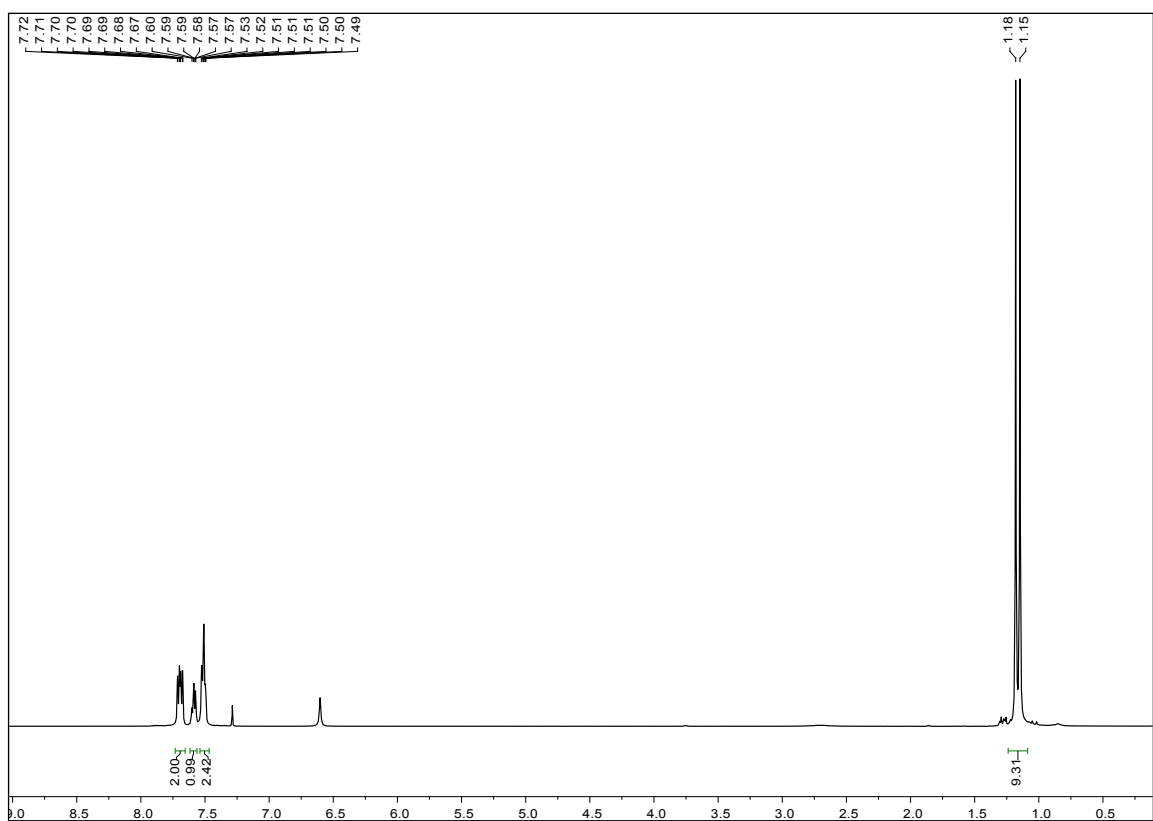
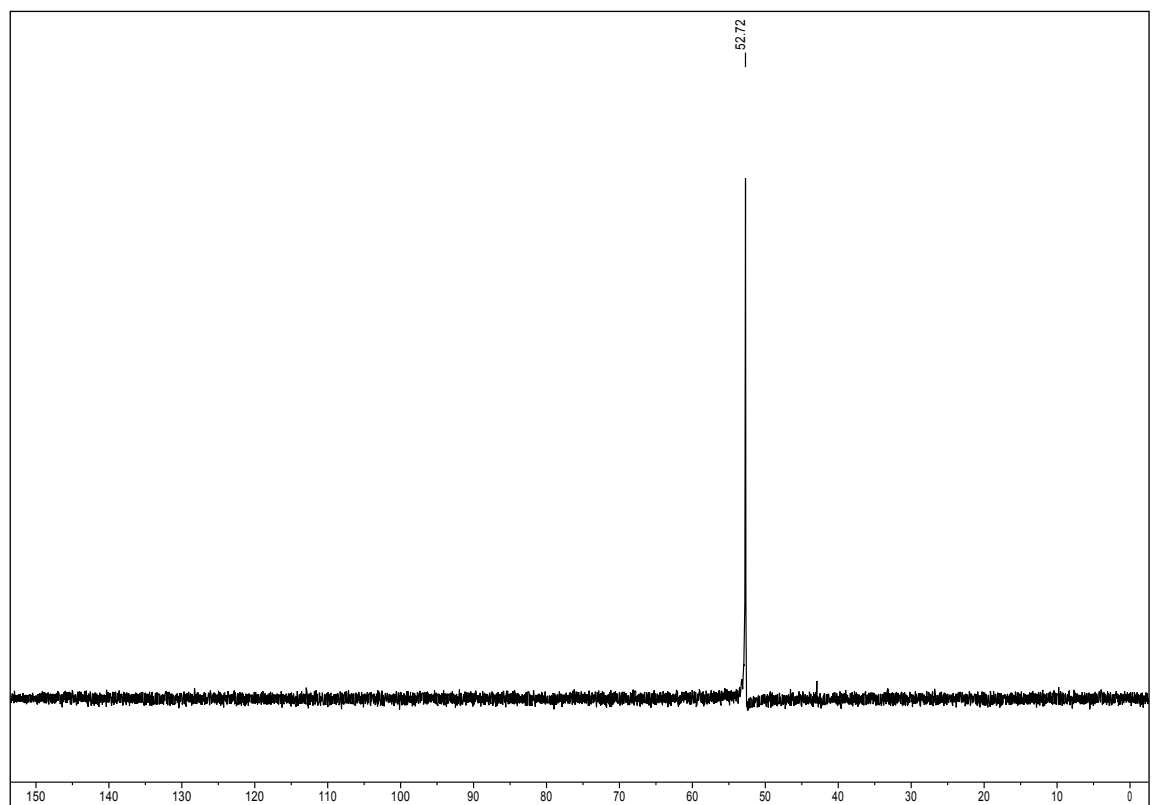
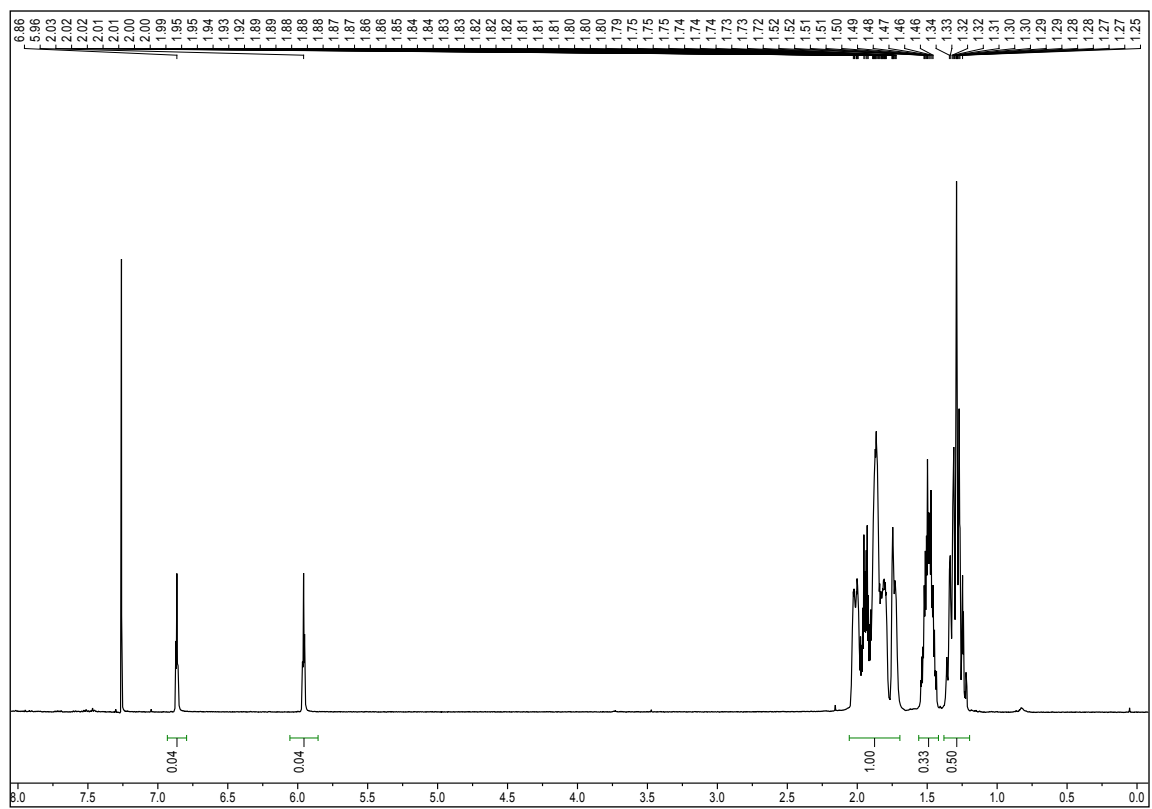


**Figure S32.** Example of CP kinetic study.  $^{13}\text{C}$  CP/MAS NMR spectra of **2** with contact time fixed between 0.5 to 30 ms.

***tert*-Butyl(phenyl)phosphine oxide (L1)**



# Dicyclohexylphosphine oxide (L3)



## 9. References

---

- <sup>1</sup> D. Massiot, F. Fayon, M. Capron, I. King, S. Le Calve, B. Alonso, J. O. Durand, B. Bujoli, Z. Gan and G. Hoatson, *Magn. Reson. Chem.*, 2002, **40**, 70–76.
- <sup>2</sup> <http://www.gosa-fit.com-about.com>
- <sup>3</sup> C. A. Busacca, J. C. Lorenz, N. Grinberg, N. Haddad, M. Hrapchak, B. Latli, H. Lee, P. Sabila, A. Saha, M. Sarvestani, S. Shen, R. Varsolona, X. Wei and C. H. Senanayake, *Org. Lett.*, 2005, **7**, 4277–4280.
- <sup>4</sup> I. Cano, L. M. Martínez-Prieto, B. Chaudret and P. W. N. M. van Leeuwen, *Chem. Eur. J.*, 2017, **23**, 1444–1450.
- <sup>5</sup> I. Cano, M. A. Huertos, A. M. Chapman, G. Buntkowsky, T. Gutmann, P. B. Groszewicz and P. W. N. M. van Leeuwen, *J. Am. Chem. Soc.*, 2015, **137**, 7718–7727.
- <sup>6</sup> (a) C. Pan, K. Pelzer, K. Philippot, B. Chaudret, F. Dassenoy, P. Lecante and M. J. Casanove, *J. Am. Chem. Soc.*, 2001, **123**, 7584–7593; (b) K. Philippot and B. Chaudret, *Oil Gas Sci. Technol. Rev. IFP*, 2007, **62**, 799–817; (c) D. González-Gálvez, P. Nolis, K. Philippot, B. Chaudret and P. W. N. M. van Leeuwen, *ACS Catal.*, 2012, **2**, 317–321; (d) E. Rafter, T. Gutmann, F. Low, G. Buntkowsky, K. Philippot, B. Chaudret and P. W. N. M. van Leeuwen, *Catal. Sci. Technol.*, 2013, **3**, 595–599.